hotpaper.net

Industrial Crops & Products 146 (2020) 112186

Contents lists available at ScienceDirect

Industrial Crops & Products

journal homepage: www.elsevier.com/locate/indcrop

Application of artificial neural network (ANN) model for prediction and optimization of coronarin D content in *Hedychium coronarium*

Asit Ray[a], Tarun Halder[b], Sudipta Jena[a], Ambika Sahoo[a], Biswajit Ghosh[b], Sujata Mohanty[c], Namita Mahapatra[d], Sanghamitra Nayak[a,*]

[a] Centre for Biotechnology, Siksha O Anusandhan (Deemed to Be University), Bhubaneswar, Odisha, India
[b] Ramakrishna Mission Vivekananda Centenary College, Rahara, Kolkata, West Bengal, India
[c] PG Department of Biotechnology, Rama Devi Women's University, Bhubaneswar, Odisha, India
[d] Regional Medical Research Centre (ICMR), Chandrasekharpur, Bhubaneswar, Odisha, India

ARTICLE INFO

Keywords:
Artificial neural network
Coronarin D
Environmental factor
Hedychium coronarium
Soil nutrients

ABSTRACT

The pharmacological properties of *Hedychium coronarium* Koen. is due to the presence of its active constituent Coronarin D. Coronarin D has been found to possess a myriad of therapeutic activities ranging from antimicrobial to anticancer. Coronarin D content in *H. coronarium* greatly differs in different habitat. In this study, an artificial neural network (ANN) based model was developed to investigate the influence of abiotic factors (climate and soil) and predict a suitable region for cultivation of *H. coronarium* with high content of coronarin D. The experimental dataset of 50 was generated by collecting *H. coronarium* rhizomes from 50 different geographical locations distributed in five different states of India. For each location, 18 input parameters were considered including soil nutrients (micronutrients and macronutrients) and climatic factors. Datasets were randomly partitioned with 72 %, 14 % and 14 % for training, validation and testing dataset, respectively. HPTLC analysis revealed coronarin D content to vary from 0.136 to 0.687 mg/100 mg dry wt among 50 *H. coronarium* rhizomes. Results showed that the multilayer perceptron (MLP) neural network with single hidden layer containing 5 neurons namely 18-5-1 structure could predict the coronarin D content accurately with a correlation coefficient (R^2) of 0.891 and root mean square error (RMSE) of 0.06. Sensitivity analysis revealed the effect of altitude, manganese and zinc on predicted coronarin D content to be slightly higher compared to other factors. The developed ANN model will assume a great significance in the prediction of the proper regions/site for optimum coronarin D yield in *H. coronarium*.

1. Introduction

Hedychium coronarium Koen. (Zingiberaceae), commonly known as white ginger lily, is a highly valued rhizomatous herb known for its medicinal and cosmetic use. It is mostly distributed in tropical countries such as India, Bangladesh, Brazil, China, Japan and South Asia (Morikawa et al., 2002; Ray et al., 2017). In India, it is distributed in Assam, Manipur, Sikkim, Peninsular and Central regions of India (Pachurekar and Dixit, 2017). The medicinal use of *Hedychium coronarium* is well documented in Indian system of traditional medicine. The rhizome is used as an excitant and carminative and for treatment of fever, diabetes, diphtheria, headache, rheumatism and inflammation (Chan and Wong, 2015; Parida et al., 2015; Ray et al., 2018). The rhizomes are also used to treat irregular menstruation, piles bleeding and urinary tract stones (Donipati and Sreeramulu, 2015). The medicinal value of *H. coronarium* is mostly due to the pharmaceutical properties of naturally occurring diterpenes in it. The rhizomes of *H. coronarium* have been used for isolation of several diterpenes having several biological efficacies such as anti-inflammatory, anti-tumor, anti-allergic, anti-malarial, leishmanicidal, analgesic and cytotoxic activities (Matsuda et al., 2002; Oh et al., 2006; Céline et al., 2009; Chimnoi et al., 2009). The pharmacologically bioactive compound of *H. coronarium* is coronarin D, a labdane diterpenoid which exhibits several biological properties such as antimicrobial, anti-inflammatory and anticancer activity (Van Kiem et al., 2011; Chen et al., 2013; Reuk-ngam et al., 2014; Lin et al., 2018; Chen et al., 2017). It inhibits nuclear factor kappa β pathway thereby inducing apoptosis and suppressing osteoclastogenesis (Kunnumakkara et al., 2008). Coronarin D exhibits excellent antifungal activity against *Candida albicans in vitro* (Kaomongkolgit et al., 2012).

* Corresponding author.
E-mail address: sanghamitran24@gmail.com (S. Nayak).

https://doi.org/10.1016/j.indcrop.2020.112186
Received 18 September 2019; Received in revised form 28 January 2020; Accepted 29 January 2020
Available online 05 February 2020
0926-6690/ © 2020 Elsevier B.V. All rights reserved.

hotpaper.net

Unavailability of high yielding coronarin D containing accessions and significant variation in the coronarin D content at different geographical regions are the main barrier for commercial production of *H. coronarium*. It is not possible to identify elite accessions of *H. coronarium* by simple chemotyping as the production of secondary metabolite are prone to vary at different habitat and environmental conditions. Study have shown environmental factors to influence the biosynthetic production of secondary metabolites (Gairola et al., 2010). Hence, it would be necessary to correlate the effect of environmental data (climatic factors and soil nutrients) of different geographical regions of Eastern India with respect to coronarin D content.

Artificial neural network (ANN) models are efficient prediction tools and yield better than conventional models (Alam and Naik, 2009). The most common type of ANN model that is being used nowadays is multilayer perceptron (MLP) (Emamgholizadeh et al., 2015). MLP is an ANN model of the feed forward type, which consists of the input layer, the hidden layer and the output layer. The MLP has many layers connected to each other, and each node is a neuron with a non-linear activation function. Perceptron calculates a single result from multiple inputs, creating a linear combination according to its inputs, and then determines the result using the non-linear transfer function (Singh et al., 2012). ANN model have also been successfully used for prediction of crop yield by using different architecture such as generalized feed forward (GFF) (Kazem and Yousif, 2017), Jordan/Elman (JE) (Michelon et al., 2018), principal component analysis (PCA) (Mohammadi and Siosemarde, 2016), and radial basis function (RBF) (Wang, 2018). ANN model have been widely used for yield prediction of some important crops such as wheat, corn, soybean, maize, potato and safflower (Abdipour et al., 2019; Ahmadi et al., 2014; Alvarez, 2009; Fieuzal et al., 2017; Matsumura et al., 2015; Moradi et al., 2013). Secondary metabolite production is influenced by a number of abiotic factors and it is very difficult to relate their associations by conventional mathematical models. ANN model has been used to predict the secondary metabolite content of plant in response to environment and soil factors. ANN prediction model have been carried out to study the effect of soil nutrients and environmental parameters on podophyllotoxin content in *P. hexandrum* (Alam and Naik, 2009), curcumin content in *C. longa* (Akbar et al., 2016) and essential oil yield in *C. longa* (Akbar et al., 2018). Therefore the present study was carried out to evaluate the predictive performance of ANN model in forecasting coronarin D content in *H. coronarium* using input environmental and soil parameters as well as to carry out sensitivity analysis of the input parameters in order to determine the most influential parameter on coronarin D content.

2. Materials and methods

2.1. Plant material and sampling locations

Hedychium coronarium accessions were sampled from fifty different geographical locations comprising five differences provinces (Assam, Andhra Pradesh, Jharkhand, Odisha and West Bengal) of Eastern India in the month of July–December 2016 at their flowering stage. From each location, three replicates plant samples were collected. To avoid collection of clonal material, samples between the replicates that were at least 15 m apart from each other were considered. The plant materials were authenticated by taxonomist Dr. P.C. Panda, Regional Plant Resource Centre, Bhubaneswar, Odisha and were deposited in the herbarium of the same institute (Table 1). The fresh rhizomes of *H. coronarium* were cut from the uprooted plants and washed in water to remove the dirt. The sampling location of 50 collected sites was determined using a GPS device (Garmin 276 C, Garmin, Olathe, KS) by measuring its latitude, longitude and altitude. Meteorological data such as precipitation, relative humidity, minimum temperature, maximum temperature and average temperature were recorded as mean/average summaries of last 5 years provided by Indian Meteorological Department (IMD) derived from facilities located close to each sampling site were recorded.

2.2. HPTLC analysis of coronarin D content

2.2.1. Preparation of extract

H. coronarium rhizomes was dried and pulverized into fine powder. Rhizome powder (10 g) was extracted with 250 ml of methanol in a Soxhlet apparatus by refluxing for 8 h. The extract was filtered, and the solvent was removed in a rotary evaporator at 50 °C and were stored at 4 °C.

2.2.2. Chromatographic conditions

HPTLC analysis of *H. coronarium* extracts were carried out in a Camag HPTLC system equipped with a Linomat V applicator, twin trough development chamber, TLC Scanner 4 equipped with the WinCATS Software 4.03. *H. coronarium* methanol extracts along with standard coronarin D were applied to the silica gel TLC aluminum $60F_{254}$ plates (Merck, India) as 6 mm band length and 1 mm apart using N2 flow with an application rate of 0.2 µl/sec. The plates were run to a distance of 85 mm in a 20 × 10 cm CAMAG® twin-trough chamber previously pre-saturated for 15 min. with mobile phase (20 ml) n-hexane: ethyl acetate (8:2). Then, it was dried under air for 5 min. Densitometry scanning was done in the absorbance-reflectance mode using deuterium lamp at 231 nm using TLC Scanner 4 (slit dimension 5 × 0.45 mm, scanning speed 20 mm/s).

2.2.3. Calibration and quantification of coronarin D

Quantification of coronarin D (Wuhan Chemfaces Biochemical Co. Ltd, Wuhan, Hubei) in *H. coronarium* extracts was carried out by external standard addition method. Stock solution of coronarin D (0.2 mg/ml) was prepared by dissolving 2 mg of coronarin D in 10 ml of chloroform. Five-point calibration curve of coronarin D was made by applying 1–5 µl of coronarin D stock solution onto TLC plate. The concentration of coronarinD in *H. coronarium* extracts was determined by plotting concentration of coronarin D in the X-axis against peak area in Y-axis.

2.3. Analysis of soil nutrients

The soils were collected at a depth of 10 − 30 cm below the surface from each location. Then the soil was dried, grounded and sieved (2 mm mesh) for the following analysis. The fine soil was used for further studies. Soil pH was measured by making a suspension of 1:2 of soil: water after stirring continuously for 30 min using a pH meter (Systronics Model no: 802). Total organic carbon content present in soil was calculated by oxidation of organic carbon with potassium dichromate (1.5 N) in an acidic environment with sulphuric acid and analyzing using spectrophotometer wet digestion (Nelson and Sommers, 1982). Total nitrogen content was calculated using the Kjeldahl method (Bremner and Mulvaney, 1982). The total potassium content was analyzed by adding 25 ml of 1 N ammonium acetate to 5 g of soil in a conical flask and shaking it for 5 min, and then the residue was filtered and tested using a photoelectric flame photometer (Systronics model no: 126). Available phosphorus in soil was measured using Bray 2 extractant method (Bray and Kurtz, 1945) method. The concentration of phosphorus was determined by plotting different concentration of standard phosphorus using a spectrophotometer (Thermo scientific evolution 201, Thermo fisher Scientific) at 660 nm. Micronutrients like Zn, Cu, Mn and Fe present in soils were measured by digesting soil: solution in the ratio of 1:2 for 2 h. The solution is a mixture of 5 mM diethylene triamine pentaacetic acid (DTPA), 0.01 M CaCl2, and 100 mM triethanolamine (TEA) with pH adjusted to 7.3 (Lindsay and Norvell, 1978). Then they were measured using an atomic absorption spectrophotometer (AAS) (Perkin Elmer Analyst 100, Perkin Elmer, USA) with absorbance wavelength set at 214, 325, 280 and 248 nm for Zn, Cu, Mn and Fe, respectively. The sulphur present in soil was

hotpaper.net

Table 1
Geographic locations and habitats characteristics of *Hedychium coronarium* populations.

S.No	Acc.	Place	District	State	Latitude	Longitude	Altitude	Voucher No
1	HC1	Rabda	Palamu	Jharkhand	23° 54′ 29.175″ N	84° 13′ 49.852″ E	325	RPRC/10626
2	HC2	Panchupandab	Nayagarh	Odisha	20° 00′ 15.415″ N	84° 53′ 26.392″ E	267	RPRC/10624
3	HC3	Chowberia	North 24 Parganas	West Bengal	22° 58′ 45.610″ N	88° 40′ 30.835″ E	11	RPRC/9566
4	HC4	Rampurhat	Birbhum	West Bengal	24° 10′ 52.961″ N	87° 46′ 52.507″ E	37	RPRC/9567
5	HC5	Rajini	Khordha	Odisha	19° 52′ 52.415″ N	84° 59′ 10.592″ E	535	RPRC/10625
6	HC6	Bolpur	Birbhum	West Bengal	23° 40′ 30.546″ N	87° 40′ 37.837″ E	58	RPRC/9569
7	HC7	Ushabali	Kandhamal	Odisha	19° 56′ 31.315″ N	83° 39′ 22.312″ E	745	RPRC/10626
8	HC8	Surampalem	Kakinada	Andhra Pradesh	17° 29′ 52.959″ N	82° 13′ 37.822″ E	341	RPRC/10798
9	HC9	Pedachama	Prakasam	Andhra Pradesh	16° 00′ 50.891″ N	78° 58′ 11.822″ E	672	RPRC/10799
10	HC10	Haroa	North 24 Parganas	West Bengal	22° 36′ 26.508″ N	88° 40′ 37.559″ E	10	RPRC/9570
11	HC11	Guma	Kandhamal	Odisha	19° 56′ 22.515″ N	83° 39′ 17.592″ E	747	RPRC/10628
12	HC12	Panitola	Tinsukia	Assam	27° 35′ 36.605″ N	95° 18′ 18.701″ E	112	RPRC/9760
13	HC13	Sargachi	Murshidabad	West Bengal	24° 10′ 52.961″ N	87° 46′ 52.507″ E	38	RPRC/9571
14	HC14	Purbagool	Hailakandi	Assam	24° 40′ 9.309″ N	92° 38′ 27.205″ E	24	RPRC/9761
15	HC15	Narendrapur	South 24 Parganas	West Bengal	22° 26′ 20.803″ N	88° 23′ 48.314″ E	58	RPRC/9565
16	HC16	Seetharampuram	Nellore	Andhra Pradesh	15° 01′ 46.879″ N	79° 05′ 06.322″ E	515	RPRC/10797
17	HC17	Raiganj	North Dinachpur	West Bengal	25° 37′ 06.706″ N	88° 07′ 32.101″ E	37	RPRC/9573
18	HC18	Judia	Keonjhar	Odisha	21° 36′ 80.621″ N	85° 33′ 26.423″ E	412	RPRC/10627
19	HC19	Lalbagh	Murshidabad	West Bengal	24° 10′ 16.746″ N	88° 16′ 35.435″ E	23	RPRC/9574
20	HC20	Chitmiti	West Singhbum	Jharkhand	22° 35′ 53.389″ N	85° 41′ 41.037″ E	737	RPRC/10642
21	HC21	Kounsi	Hazaribag	Jharkhand	23° 47′ 34.384″ N	85° 22′ 41.117″ E	508	RPRC/10631
22	HC22	Krishnanagar	Nadia	West Bengal	23° 24′ 03.148″ N	88° 30′ 05.026″ E	19	RPRC/10630
23	HC23	Simlipal	Mayurbhanj	Odisha	21° 35′ 35.214″ N	86° 48′ 20.157″ E	816	RPRC/10629
24	HC24	Deogada	Kandhamal	Odisha	19° 55′ 08.918″ N	83° 37′ 65.603″ E	681	RPRC/10637
25	HC25	Ghonza	North 24 Parganas	West Bengal	22° 37′ 00516″ N	88° 24′ 10.422″ E	7	RPRC/9575
24	HC24	Deogada	Kandhamal	Odisha	19° 55′ 08.918″ N	83° 37′ 65.603″ E	681	RPRC/10638
25	HC25	Ghonza	North 24 Parganas	West Bengal	22° 37′ 00516″ N	88° 24′ 10.422″ E	7	RPRC/9576
26	HC26	Sokra	Palamu	Jharkhand	23° 57′ 17.008″ N	84° 04′ 06.597″ E	322	RPRC/10635
27	HC27	Tidipadar	Kandhamal	Odisha	19° 54′ 33.682″ N	83° 38′ 48.526″ E	901	RPRC/10639
28	HC28	Baramunda	Khurdha	Odisha	20° 16′ 16.223″ N	85° 47′ 39.627″ E	44	RPRC/10640
29	HC29	Nayapalli	Khurdha	Odisha	20° 17′ 53.807″ N	85° 48′ 11.618″ E	59	RPRC/10641
30	HC30	Gimli	Visakhapatnam	Andhra Pradesh	18° 00′ 03.764″ N	82° 29′ 13.339″ E	350	RPRC/10800
31	HC31	G. Madagulla	Visakhapatnam	Andhra Pradesh	17° 55′ 54.287″ N	82° 32′ 03.416″ E	981	RPRC/10801
32	HC32	Barpathar	Golaghat	Assam	26° 27′ 3.463″ N	93° 56′ 54.912″ E	103	RPRC/9758
33	HC33	Konnagar	Hooghly	West Bengal	22° 42′ 33.593″ N	88° 18′ 42.415″ E	7	RPRC/9577
34	HC34	Jirighat	Cachar	Assam	24° 48′ 28.102″ N	93° 06′ 28.091″ E	36	RPRC/9759
35	HC35	Lalpani	Cachar	Assam	24° 47′ 09.752″ N	93° 05′ 28.091″ E	31	RPRC/9763
36	HC36	Palpara	Nadia	West Bengal	23° 04′ 02.249″ N	88° 31′ 17.326″ E	10	RPRC/9578
37	HC37	Tarapith	Birbhum	West Bengal	24° 06′ 50.558″ N	87° 47′ 56.687″ E	33	RPRC/9579
38	HC38	Bolpur	Birbhum	West Bengal	23° 40′ 07.281″ N	87° 40′ 57.963″ E	51	RPRC/9580
39	HC39	Diphu	Karbi anglong	Assam	25° 50′ 47.884″ N	93° 25′ 47.506″ E	192	RPRC/9762
40	HC40	Muchisha	South 24 Parganas	West Bengal	22° 23′ 48.342″ N	88° 11′ 37.535″ E	9	RPRC/9581
41	HC41	Talakona	Chittor	Andhra Pradesh	13° 48′ 42.342″ N	79° 10′ 37.503″ E	777	RPRC/10803
42	HC42	Bangaria	Nadia	West Bengal	23° 35′ 13.614″ N	88° 26′ 03.395″ E	24	RPRC/9582
43	HC43	Kadu	Kalahandi	Odisha	20° 20′ 38.331″ N	83° 53′ 40.885″ E	598	RPRC/10637
44	HC44	Rachapalli	East Godavari	Andhra Pradesh	14° 27′ 54.962″ N	79° 10′ 6.667″ E	452	RPRC/10804
45	HC45	Jargo	Ranchi	Jharkhand	22° 56′ 16.236″ N	85° 45′ 42.667″ E	418	RPRC/10632
46	HC46	Morabadi	Ranchi	Jharkhand	23° 24′ 02.864″ N	85° 20′ 16.486″ E	668	RPRC/10633
47	HC47	Karimpur	Nadia	West Bengal	23° 58′ 27.472″ N	88° 37′ 35.571″ E	22	RPRC/9583
48	HC48	R. Udayagiri	Gajapati	Odisha	19° 09′ 33.972″ N	84° 09′ 38.571″ E	631	RPRC/10634
49	HC49	Padmapur	Gajapati	Odisha	19° 14′ 16.472″ N	83° 49′ 11.552″ E	130	RPRC/10636
50	HC50	Lataguri	Jalpaiguri	West Bengal	26° 43′ 15.889″ N	88° 46′ 15.251″ E	122	RPRC/9584

digested using $Mg(NO_3)_2$ and HNO_3 and measured by barium sulfate turbidimetric method (Page et al., 1982).

2.4. Artificial neural network model development

In the current research, artificial neural-network (ANN) model was implemented with Statistica 7 package (Stat Soft Inc.) using feed forward back propagation (BP) method and trained using the climatic and edaphic factors as the input and coronarin D content as the output variables. The topology of ANN structure is composed of 18 independent variables as input and one dependent variable as output to generate 18:1 pattern. Eighteen independent variables, *i.e.*, altitude, precipitation, maximum temperature, minimum temperature, average annual temperature, average relative humidity, pH, electrical conductivity, organic carbon, nitrogen, phosphorus, potassium, manganese, zinc, iron, boron, copper and sulphur content. Coronarin D content was selected as output for modeling of ANN.

In this study, a total of 50 samples were randomly divided into 3 datasets namely, training, validation, and testing. Data were randomly partitioned with 72 % (36 samples) for training, 14 % (7 samples) for validation and 14 % (7 samples) for the testing dataset. Following training, the ANN was validated and tested with the validation and testing data set to evaluate the prediction performance of the final ANN models. In the current research, neurons in the range of 2–17 were taken for analysis based on hit and trial. The neurons were optimized to get the best prediction performance. The flow of data occurs from the input layer to the hidden layer and is then distributed to the output layer. Throughout the training process, the connection weights and biases were adjusted to minimize the difference between the experimental and predicted values. The neurons there in the hidden or output layer acts as summing junction which joins and adjust the inputs from the preceding layer using the formula:

hotpaper.net

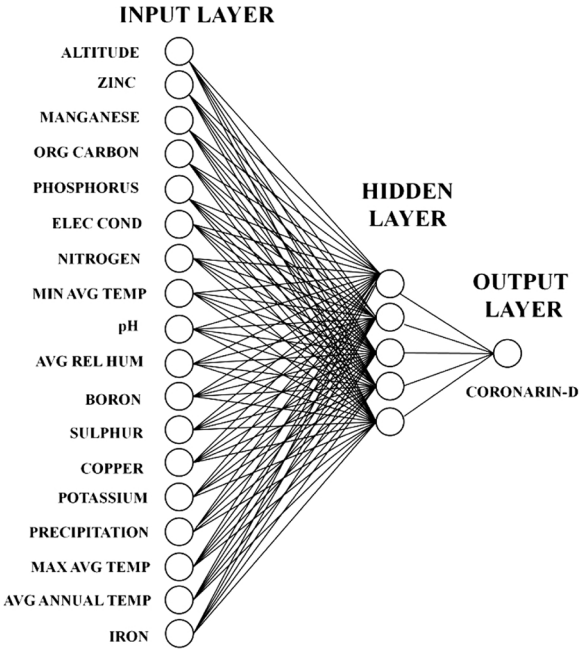

Fig. 1. Architecture of the multilayer perceptron feed forward network used in the study.

Table 2
Actual and predicted coronarin D content of training dataset.

Acc No	Predicted coronarin D content	Actual coronarin D content	Absolute error	Absolute percentage error
HC1	0.321	0.349	0.028	2.80
HC3	0.307	0.264	0.043	4.30
HC4	0.208	0.216	0.008	0.80
HC5	0.562	0.438	0.124	12.4
HC6	0.172	0.223	0.051	5.10
HC7	0.526	0.460	0.066	6.60
HC8	0.304	0.270	0.034	3.40
HC9	0.581	0.485	0.096	9.60
HC10	0.164	0.265	0.101	10.1
HC11	0.513	0.515	0.002	0.20
HC12	0.497	0.537	0.040	4.00
HC13	0.225	0.219	0.006	0.60
HC15	0.286	0.350	0.064	6.40
HC18	0.281	0.318	0.037	3.70
HC20	0.519	0.498	0.021	2.10
HC21	0.371	0.443	0.072	7.20
HC22	0.265	0.190	0.075	7.50
HC24	0.497	0.566	0.069	6.90
HC25	0.154	0.257	0.103	10.30
HC26	0.187	0.227	0.040	4.00
HC27	0.567	0.554	0.013	1.30
HC28	0.231	0.255	0.024	2.40
HC31	0.341	0.445	0.104	10.40
HC32	0.687	0.635	0.052	5.20
HC33	0.562	0.511	0.051	5.10
HC34	0.631	0.653	0.022	2.20
HC35	0.589	0.655	0.066	6.60
HC36	0.231	0.215	0.016	1.60
HC37	0.211	0.215	0.004	0.40
HC38	0.237	0.227	0.010	1.00
HC39	0.687	0.623	0.064	6.40
HC41	0.541	0.446	0.095	9.50
HC43	0.481	0.497	0.016	1.60
HC44	0.223	0.285	0.062	6.20
HC47	0.215	0.220	0.005	0.50
HC48	0.621	0.549	0.072	7.20
Mean			0.048	4.87

Table 3
Actual and predicted coronarin D content of testing dataset.

Acc No	Predicted coronarin D content	Actual coronarin D content	Absolute error	Absolute percentage error
HC2	0.262	0.286	0.024	2.40
HC16	0.388	0.434	0.046	4.60
HC17	0.216	0.261	0.045	4.50
HC29	0.167	0.337	0.170	17.00
HC45	0.592	0.479	0.113	11.30
HC49	0.187	0.315	0.128	12.80
HC50	0.311	0.326	0.015	1.50
Mean			0.077	7.73

Table 4
Actual and predicted coronarin D content of validation dataset.

Acc No	Predicted coronarin D content	Actual coronarin D content	Absolute error	Absolute percentage error
HC14	0.811	0.683	0.128	12.8
HC19	0.033	0.054	0.021	2.10
HC23	0.989	0.881	0.108	10.8
HC30	0.884	0.823	0.061	6.10
HC40	0.111	0.142	0.031	3.10
HC42	0.076	0.136	0.060	6.00
HC46	0.546	0.537	0.009	0.90
Mean			0.059	5.97

$$y_s=\sum_{t=1}^{p} v_s u_{st}+x_t$$

where y_s is the input to node t in hidden or output layer, s is the number of nodes, v_s is the output of the preceding layer, u_{st} is the weight interconnection in between the s and t node and x_t is the bias connected with node t.

The developed neural-network model utilizes a sigmoidal transfer function to measure the nonlinear relationship. The transfer function is computed by the following formula:

$$W_t=\frac{1}{1+e^{-ys}}$$

Where, W_t is the output of node t. Considering, the fact that sigmoid transfer function lies between 0 and 1, in order to avoid over-fitting, input and output variables were also scaled to the range of 0–1 by the following formula:

$$B_{norm} = (B\text{-}B_{min})/(B_{max} - B_{min})$$

Where, B_{norm} is the normalized value, B is the actual value, B_{min} is the minimum value and B_{max} is the maximum value. In order to get the actual value, the output values are again denormalized.

The prediction performance of the developed model was measured by computing correlation coefficient (R^2), root mean square error (RMSE), mean absolute error (MAE) and mean absolute percentage error (MAPE) values as follows.

$$\mathbf{R^2} = 1 - \frac{\sum_{i=1}^{n} (x_i - x_{ik})^2}{\sum_{i=1}^{n} (x_{ik} - x_z)^2}$$

$$\mathbf{RMSE} = \frac{1}{n}\sum_{i=1}^{n} (x_i - x_{ik})^2$$

$$\mathbf{MAE} = \frac{1}{n}\sum_{i=1}^{n} |x_i - x_{ik}|$$

$$\mathbf{MAPE} = \frac{1}{n}\sum_{i=1}^{n} \left|\frac{x_i - x_{ik}}{x_i}\right| \times 100\%$$

hotpaper.net

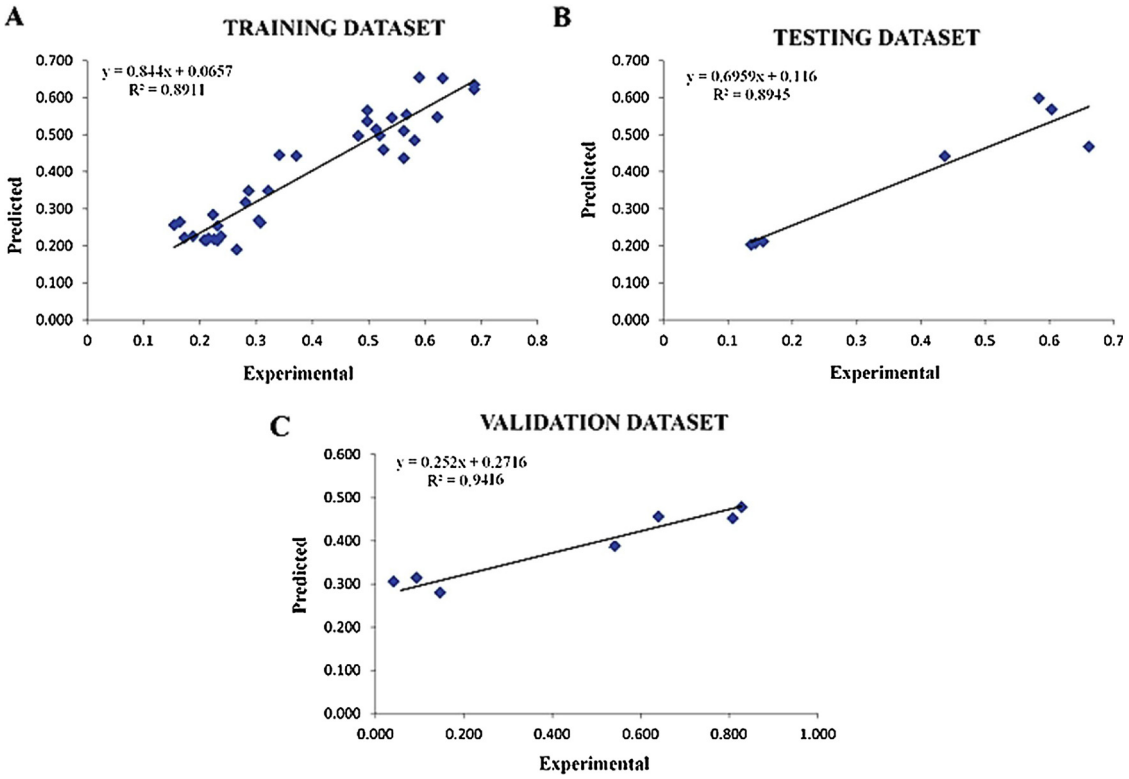

Fig. 2. Scatter plot showing experimental and predicted value of coronarin D content of (A) training; (B) testing and (C) validation data.

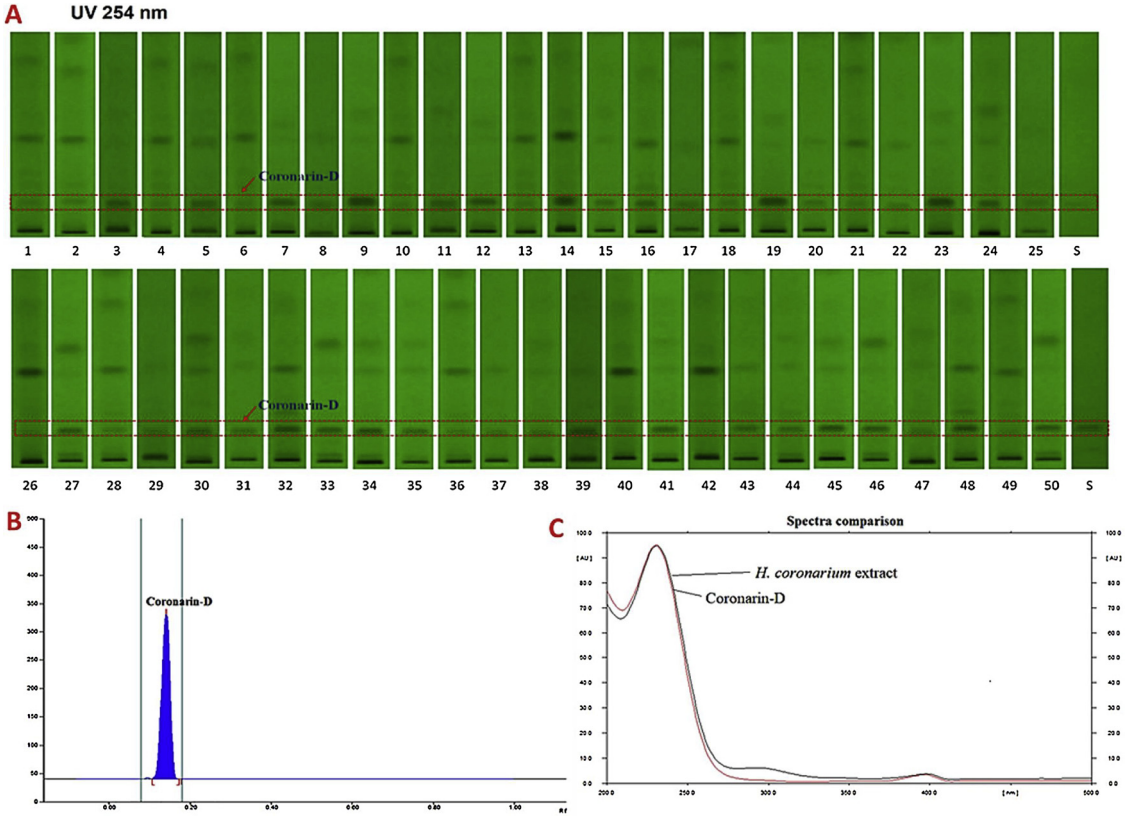

Fig. 3. HPTLC analysis of coronarin D in *H. coronarium*. (A) TLC plate at 254 nm. (Samples 1-50: *H. coronarium* accessions; S = Reference coronarin D); (B) Standard coronarin D and (C) Overlay UV spectra of standard coronarin D and extract.

hotpaper.net

Table 5
Recovery study of coronarin D.

Acc No	Coronarin D + extract (μg)	Coronarin D (μg)	Coronarin D in extract (μg)	% Recovery
HC1	0.55	0	0.55	100
HC1 + 0.2	0.75	0.2	0.74	98.66
HC1 + 0.4	0.95	0.4	0.97	102.1
HC1 + 0.6	1.15	0.6	1.14	99.13
Average				99.96

Table 6
Repeatability study of coronarin D.

Acc No	Peak area						Avg. area	SD	%RSD
	1	2	3	4	5	6			
HC1	2431	2429	2440	2427	2436	2422	2430.8	6.4	0.26
HC2	1789	1793	1781	1789	1772	1796	1786.7	8.8	0.49
HC3	2170	2186	2193	2182	2179	2171	2180.2	8.8	0.40

Where, x_i is predicted value, x_{ik} is the experimental value, x_z is the mean of experimental value and n is the number of observations.

2.5. Sensitivity analysis

Sensitivity analysis was carried out to identify the individual eff ;ects of each of the input variables on predicted coronarin D content. The sensitivity test was performed for ANN model without a specific input variable, and the eff ;ects of the input variables to predict coronarin D content in ANN model was ranked from the highest to lowest. The variable with higher error ratios indicate more important parameters (Miller et al., 2019).

3. Results

3.1. Development of ANN model for optimization of coronarin D content

The architecture of neural network model comprises of 18 input neurons and one output neuron (Fig. 1). The feed forward network uses back propagation algorithm by updating the weights thereby minimizing the squared error between the experimental output values and the predicted output values. Selecting appropriate network size is essential for getting a good ANN model. Less number of neurons present in the hidden layer may have an effect on the performance of ANN model. An increased number of hidden layer neurons will lead to overfitting issues, namely the conditions in which the error would be small for the training dataset but very large for the test dataset. This is due to the fact that higher the number of neurons, the more complex the fitted functions. Therefore in the present study network were tested with neurons in the range of 3–16. The best number of hidden layers and number of neurons in hidden layers are determined by trial and error and based on the highest correlation coefficient and lowest obtained error. The network with single hidden layer and 5 neurons in the hidden layer was selected as the best fit ANN model as it displayed the lowest error and highest correlation coefficient. The analysis showed that multilayer perceptron (MLP) network have outstanding nonlinear relationship between input and output. Normal, the best performance model is selected as the model having least root mean square (RMSE) values and high coefficient of determination between experimental and predicted values. Theoretically an ideal model RMSE values should be near to 0 and coefficient of determination (R^2) should be 1. The training, testing and validation RMSE values for 18-5-1 network structure were 0.06, 0.09 and 0.20 thereby indicating that the build model is appropriate. The result comparison of actual and predicted values of training, testing and validation dataset is provided in Tables 2–4, respectively. The linear plot generated in training process for experimental and predicted values showed a coefficient of determination (R^2) value of 0.891, thereby implying that the training process is accurate (Fig. 2A). The linear plot generated in testing process for experimental and predicted values of coronarin D content showed a coefficient of determination (R^2) value of 0.894, thereby implying that the testing process is highly precise (Fig. 2B). The validation dataset comparison of experimental and predicted values displayed a coefficient of determination (R^2) value of 0.942, thereby indicating the accuracy of the validation process (Fig. 2C).

Table 7
Climatic data for 50 *H. coronarium* accessions from different geographical regions of Eastern India.

SI No	Acc.	Precipitation (mm)	Max. Temp. (°C)	Min. Temp. (°C)	Avg. Temp. (°C)	Avg. Rel. Hum. (%)	Altitude (m)
1	HC1	1091	38.2	9	25.4	57	325
2	HC2	1346	35.4	15.2	27	69	267
3	HC3	1569	36.4	12.4	26.4	75	11
4	HC4	1400	36.9	11.4	26.2	77	37
5	HC5	1266	33.2	16.3	28.1	76	535
6	HC6	1287	35.9	12	26.3	75	58
7	HC7	1340	37.5	12.1	25.06	62	745
8	HC8	1109	37.1	18.9	27.8	75	341
9	HC9	825	38.2	19.6	28.5	56	672
10	HC10	1527	35.6	12.3	26.3	75	10
11	HC11	1328	37	11.8	24	62	747
12	HC12	2679	31.1	9.7	23.1	82	112
13	HC13	1344	37.4	11.7	26.2	77	38
14	HC14	3075	31.9	11.7	24.9	78	24
15	HC15	1735	35.9	12.6	26.2	74	58
16	HC16	753	40.1	19	29.2	70	515
17	HC17	1570	35	9.9	24.9	76	37
18	HC18	1295	37.7	11.2	24.8	71	412
19	HC19	1343	37.3	11.7	26.2	77	23
20	HC20	1279	40.4	11.7	26.3	64	737
21	HC21	1274	37.9	9.5	23.7	63	508
22	HC22	1353	37.7	11.2	26.4	75	19
23	HC23	1596	38	13.4	26.8	71	816
24	HC24	1335	37.4	12.3	24.1	61	681
25	HC25	1568	35.3	12.3	26.3	74	7
26	HC26	1146	41.2	9.2	25.4	58	322
27	HC27	1345	36.8	12	24.71	63	901
28	HC28	1505	36.1	15.7	27.4	76	44
29	HC29	1520	36.3	15.8	27.2	77	59
30	HC30	1270	32.8	13	23.1	75	350
31	HC31	1290	32.4	12.8	22.8	76	981
32	HC32	1960	32.4	9.8	24	82	103
33	HC33	1175	37.5	12.8	26.5	75	7
34	HC34	3144	32.2	11.6	24.9	77	36
35	HC35	2996	32.2	11.4	24.9	78	31
36	HC36	1320	38	11.6	26.3	76	10
37	HC37	1389	38.1	11.5	26.3	64	33
38	HC38	1287	38	12	26.3	65	51
39	HC39	1453	32.4	9.1	24	78	192
40	HC40	1592	33.5	14.3	26.2	75	9
41	HC41	862	37.8	17.7	27.4	71	777
42	HC42	1299	37.8	11.5	26.4	74	24
43	HC43	1253	39.4	13.6	26.7	69	598
44	HC44	1115	37.8	18.5	27.9	69	452
45	HC45	1397	35.9	9.9	23.7	60	418
46	HC46	1432	36	10.1	23.8	61	668
47	HC47	1434	37	11.5	26.1	75	22
48	HC48	1272	34.4	16.6	23.2	75	631
49	HC49	1285	34.3	16.5	26.7	76	130
50	HC50	3242	30.9	10.6	24	64	122

Max. Temp.: Maximum temperature, Min. Temp.: Minimum temperature, Avg. Temp.: Average temperature, Avg. Rel. Hum. : Average relative humidity.

hotpaper.net

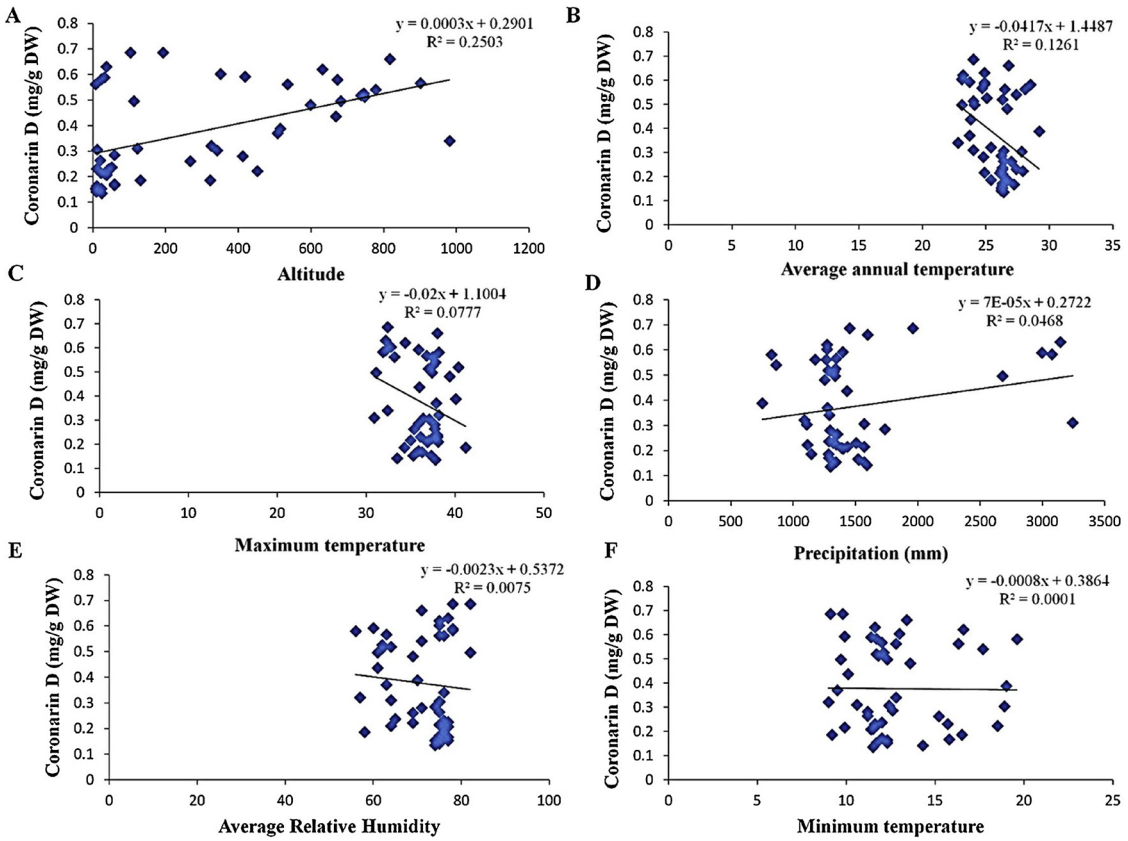

Fig. 4. Scatter plot matrix showing correlation of different environmental parameters with coronarin D content. (A) Altitude; (B) Average annual temperature; (C) Maximum temperature; (D) Precipitation; (E) Average relative humidity and (F) Minimum temperature.

Table 8
p and r value of different factors.

Factors	r-value	p-value	Factors	r-value	p-value
Precipitation	0.131	0.216	Nitrogen	0.292	0.039
Max temp	0.279	0.050	Phosphorus	0.144	0.319
Min temp	0.012	0.936	Potassium	0.435	0.002
Average annual temperature	0.355	0.011	Sulphur	0.334	0.018
Average relative humidity	0.087	0.549	Boron	0.119	0.409
Altitude	0.500	0.0002	Iron	0.502	0.0002
pH	0.261	0.067	Zinc	0.182	0.205
Electrical Conductivity	0.221	0.123	Manganese	0.533	0.0001
Organic Carbon	0.043	0.764	Copper	0.476	0.0004

3.2. Analysis of parameters

3.2.1. Coronarin D content

A total of fifty *H. coronarium* accessions were sampled from various geographical locations of Eastern India. The processing of all the extracts was carried out in a similar fashion and analysis of coronarin D was done using HPTLC. Various mobile phases were tested using different solvents in different ratio. The mobile phase consisting of n-hexane: ethyl acetate was used in the ratio 8:2 as it gave a compact band for coronarin D with a R_f (Retardation factor) of 0.20 ± 0.02 with a good resolution. The TLC photo documentation of *H. coronarium* extract and coronarin D at 254 nm is shown in Fig. 3A. The HPTLC chromatogram of reference coronarin D is shown in Fig. 3B. The spectrum analysis corresponding to this peak was also found to overlay exactly, indicating the compound at R_f value of 0.20 in standard and the sample. Both the extract and standard showed absorbance maxima at 231 nm (Fig. 3C). Calibration curve of coronarin D was generated, and the method was validated in terms of repeatability, recovery, robustness, limit of detection (LOD), and limit of quantification (LOQ) parameters. Calibration curve of coronarin D was generated, and the method was validation was carried out by measuring repeatability, recovery, robustness, LOD, and LOQ parameters. The calibration curve showed linearity in between 200 − 1000 ng/spot for coronarin D. It was represented by the regression equation y = 21.218 + 0.232x, where y = peak area and x = concentration of coronarin D. The correlation coefficient (R^2) is 0.9987 thereby representing strong linear relationship between concentration of analyte and peak area. Recovery studies were carried out by the adding standard coronarin D (0.2, 0.4 and 0.6 µg) to the already analyzed *H. coronarium* extract. The average recovery percentage of coronarin D at three different concentrations was found to be 99.96 % (Table 5). Method robustness was assessed by slightly varying the solvents proportion in the mobile phase and by changing the developing distance. Mobile phases with slightly varying compositions *viz.*, 20 ml of n-hexane: ethyl acetate (7.5:2:5; 8:2; 8.5:1.5), were used and the migration distances were also varied between 70, 75 and 80 mm. No variation in the peak areas was seen. Repeatability was measured by repeated application of sample solution onto the TLC plate and scanning the spot six times and measuring its peak area. The relative standard deviation (RSD) of the peak area was found to be less than 1 % (Table 6).

Method sensitivity was assessed by measuring its LOD and LOQ where

$$LOD = 3.3 \times (SD/S)$$

and

$$LOQ = 10 \times (SD/S)$$

SD = standard deviation and S = slope of the calibration curve. The LOD and LOQ for coronarin D were found to be 35 and 115 ng/spot, respectively.

Coronarin D content in *H. coronarium* varied from a minimum of

hotpaper.net

Table 9
Physicochemical properties of soil samples collected from different geographical locations of Eastern India.

S.No	Acc.	pH	E.C (dS/m)	O.C. (%)	N_2 (kg/ha)	P_2O_5 (kg/ha)	K_2O (kg/ha)	S (mg/kg)	B (mg/kg)	Fe (mg/kg)	Zn (mg/kg)	Mn (mg/kg)	Cu (mg/kg)
1	HC1	6.6	0.47	0.76	285	13.2	187	23.2	1.3	10.5	1.34	17.23	1.31
2	HC2	4.6	1.33	0.51	230	9.5	135	16.8	0.75	5.7	1.89	2.68	1.22
3	HC3	7.4	0.86	0.79	214	31.5	143	12.3	0.94	39.2	0.96	10.24	1.61
4	HC4	6.2	0.77	0.83	205	28.6	162	9.42	0.89	31.7	1.1	18.57	1.56
5	HC5	4.8	1.61	0.39	241	12.3	112	15.37	0.81	7.8	0.58	5.12	1.19
6	HC6	6.1	0.71	0.75	195	33.2	139	8.97	0.82	29.1	0.87	17.91	1.68
7	HC7	4.6	0.97	0.48	226	10.7	394	18.21	0.86	8.1	1.65	3.46	1.28
8	HC8	6.2	0.65	0.42	135	32.3	306	16.56	0.48	11.4	2.23	6.14	0.46
9	HC9	6.8	0.52	0.47	157	30.8	297	19.13	0.53	8.9	0.47	5.67	0.52
10	HC10	7.8	0.92	0.8	223	26.4	124	11.14	0.76	30.1	1.05	12.19	1.48
11	HC11	4.8	0.82	0.53	212	11.8	387	17.33	0.79	6.9	1.36	2.48	1.17
12	HC12	7.2	0.58	0.49	268	20.2	313	19.64	1.19	15.4	0.72	6.57	0.62
13	HC13	7.6	0.81	0.71	227	27.1	167	7.99	0.69	38.1	1.02	19.35	1.49
14	HC14	7.1	0.63	0.8	286	23.8	134	16.49	0.57	17.9	0.89	4.49	0.57
15	HC15	4.8	0.69	0.44	295	13.4	198	19.64	0.87	28.4	1.42	8.82	1.42
16	HC16	6.9	0.59	0.36	162	29.7	271	18.71	0.59	12.1	0.41	3.36	0.83
17	HC17	7.3	0.87	0.69	233	34.3	121	7.21	1.09	40.9	1.38	11.14	1.32
18	HC18	6.3	1.4	0.55	204	8.6	106	6.98	0.62	9.7	0.49	2.38	1.23
19	HC19	7.6	0.82	0.6	211	30.8	202	8.36	0.69	43.6	1.13	18.52	1.37
20	HC20	4.6	0.91	0.78	312	8.9	189	6.11	0.89	14.1	0.97	13.38	1.18
21	HC21	5	0.41	0.86	297	9.7	202	5.98	1.45	11.2	1.41	9.67	1.19
22	HC22	7.7	0.82	0.63	178	29.8	126	7.76	0.61	38.5	1.16	17.29	1.51
23	HC23	5.4	0.68	0.6	196	13.4	151	6.54	0.59	2.3	0.63	3.11	1.25
24	HC24	5.3	0.81	0.58	216	12.9	412	13.38	0.79	6.7	0.71	2.54	1.19
25	HC25	7.8	0.86	0.77	205	27.9	117	12.29	0.87	28.6	1.12	12.21	1.43
26	HC26	6.7	0.47	0.8	291	12.6	169	22.34	1.37	9.8	1.39	16.33	1.28
27	HC27	4.7	0.74	0.65	237	10.6	441	15.31	0.66	4.8	1.48	3.67	1.21
28	HC28	5.1	1.52	0.32	223	12.9	137	15.86	0.83	7.9	0.76	1.97	1.12
29	HC29	5.3	1.41	0.37	217	11.5	145	16.27	0.49	11.4	0.82	2.66	1.18
30	HC30	4.8	0.63	0.81	137	34.6	302	16.92	0.41	9.1	1.92	6.86	0.87
31	HC31	5	0.71	0.77	148	27.9	287	17.34	0.49	9.8	2.06	7.31	0.96
32	HC32	6.9	0.49	0.58	312	26.7	307	15.69	0.62	16.5	0.77	4.59	0.62
33	HC33	6.1	0.92	0.87	219	28.25	193	8.81	1.22	42.8	1.57	13.25	1.31
34	HC34	7	0.58	0.77	337	30.4	292	16.82	0.67	18.3	0.65	5.67	0.57
35	HC35	6.6	0.64	0.83	351	31.4	326	16.27	0.71	15.2	0.83	4.28	0.69
36	HC36	7.8	0.61	0.66	187	26.5	167	7.46	0.73	34.7	0.93	16.38	1.52
37	HC37	6.3	0.83	0.78	202	29.4	181	8.39	0.81	41.4	0.81	16.97	1.39
38	HC38	6	0.74	0.81	210	26.3	206	5.12	0.69	27.2	0.79	18.51	1.43
39	HC39	6.8	0.41	0.52	325	19.8	378	17.73	0.74	17.7	0.61	6.11	1.58
40	HC40	4.4	0.88	0.38	293	11.6	218	14.67	0.82	35.7	1.37	10.24	1.62
41	HC41	6.9	0.59	0.44	152	25.8	94	19.37	0.59	11.2	0.55	5.73	0.36
42	HC42	7.7	0.79	0.54	202	26.2	134	6.47	0.78	29.2	0.87	19.16	1.67
43	HC43	5.3	1.26	0.63	231	13.5	124	15.88	0.84	6.3	0.57	3.28	0.21
44	HC44	6.2	0.72	0.49	163	27.15	315	18.16	0.55	10.7	2.51	4.61	0.43
45	HC45	5.4	0.43	0.92	315	13.7	117	19.25	0.74	9.1	1.48	8.35	1.22
46	HC46	5.2	0.4	0.89	305	11.95	133	17.74	0.61	10.7	1.67	13.22	1.13
47	HC47	7.7	0.56	0.59	196	28.2	182	11.53	0.69	33.1	1.07	19.37	1.46
48	HC48	6	1.34	0.57	205	14.4	162	14.62	1.16	5.9	1.31	2.66	1.24
49	HC49	6.1	1.69	0.6	227	12.7	143	13.38	1.04	7.2	1.62	2.19	1.09
50	HC50	6.3	0.52	0.81	187	27.1	166	6.49	0.83	36.9	0.79	17.05	1.69

E.C., Electrical conductivity, O.C., Organic carbon.

0.136 mg/100 mg dry wt (HC42) to a maximum of 0.687 mg/100 mg, dry wt (HC32). The average coronarin D content of these 50 accessions were 0.377 ± 0.178 mg/100 mg, dry wt.

3.2.2. Influence of altitude

The elevation of 50 sampling accessions of *H. coronarium* ranged from 7 m (HC33) to 981 m (HC31) above sea level (Table 7). The content of coronarin D increased with increase in elevation as shown in scatter plot (Fig. 4A). The correlation coefficient (r) was 0.50 at significance level $p < 0.01$ (Table 8), which showed that coronarin D increased with increase in altitude.

3.2.3. Influence of environmental factors

The environmental factors showed a higher degree of variation among 50 collected accessions used in the present study. The wide variation in environmental factors might be due to the fact that samples were collected from diverse geographical locations. The environmental variables used in the present study were precipitation, maximum temperature, minimum temperature, average annual temperature and average relative humidity and its relationship with coronarin D content is shown as scatter plot in Fig. 4B–F. The precipitation ranged from 753 to 3242 mm in a year, maximum temperature recorded varied from 30.9 to 41.2 °C, minimum temperature recorded varied from 9 to 19.6 °C. The average annual temperature range from 22.8 to 29.2 °C, whereas average relative humidity varied from 56 to 82 %. The coronarin D content showed positive significant relationship with average annual temperature ($r = 0.355$), maximum temperature ($r = 0.279$) at five percent level of significance. However, precipitation, average relative humidity and minimum temperature exhibited positive correlation with coronarin D content without any significance (Table 8).

3.2.4. Influence of soil factors

Soil parameters such as pH, electrical conductivity, organic carbon, macronutrients and micronutrients showed a large extent of variation

hotpaper.net

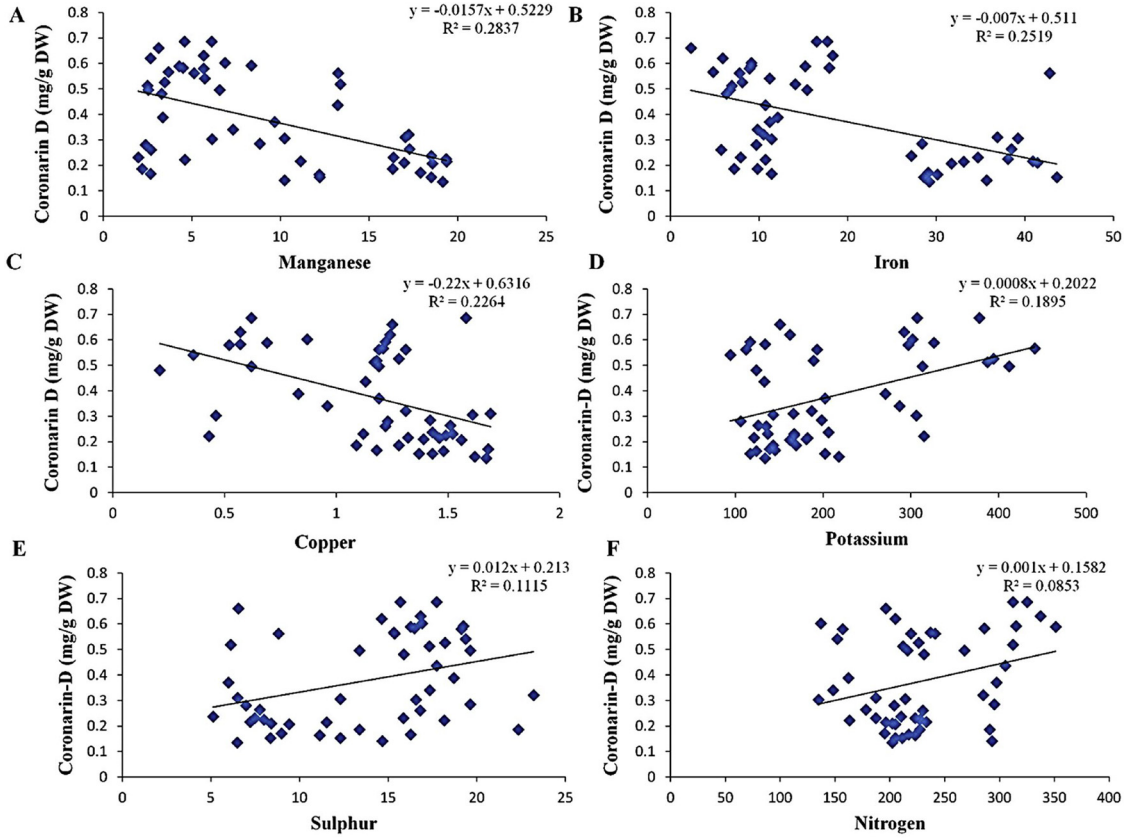

Fig. 5. Scatter plot matrix showing correlation of different soil nutrients with coronarin D content. (A) Manganese; (B) Iron; (C) Copper; (D) Potassium; (E) Sulphur and (F) Nitrogen.

among sampling sites from where plant samples were collected (Table 9). The differences in soil characteristics might be due to the fact that samples were collected from different geographical areas having different terrain and climatic conditions. The linear relationship between different soil factors with coronarin D content is shown as scatter plot in Fig. 5 and 6. Soil pH varied from 4.4 (medium acidic) to 7.8 (slightly basic) among collected soil samples. The electrical conductivity measured for soils varied from 0.4 to 1.69 dS/m. Soil Organic carbon content ranged from 0.32 to 0.92 %. Macronutrients such as nitrogen, phosphorus and potassium varied from 135 to 351, 8.6 to 34.6 and 94 to 441 kg/ha, respectively. Micronutrients such as sulphur, boron, iron, zinc, manganese and copper in soil ranged from 5.12 to 23.2, 0.41 to 1.45, 2.3 to 43.6, 0.41 to 2.51, 1.97 to 19.37 and 0.21 to 1.69 mg/kg, respectively. The coronarin D content showed positive and significant correlation with manganese ($r = 0.533$), iron ($r = 0.502$), copper ($r = 0.476$), potassium ($r = 0.432$), sulphur ($r = 0.334$), nitrogen ($r = 0.292$) at five percent level of significance. However electrical conductivity, pH, zinc, boron, phosphorus and organic carbon exhibited positive correlation with coronarin D content without any significant difference.

3.3. Response surface plots

The response surface plot of moderate and highly sensitive parameters were plotted to understand the impact of the different parameters and find out the optimal level of each parameter for obtaining high coronarin D content. The interaction between altitude and various soil parameters such pH, nitrogen, zinc, iron and manganese have been illustrated as response surface plots. Higher coronarin D content was observed in places with low iron content (< 10 mg/kg) and high altitude (> 500 m) (Fig. 7A). The decrease in coronarin D content was more significant when the iron content exceeded 35 mg/kg. Similarly the content of coronarin D increased when the nitrogen content in the soil exceeded 340 mg/kg and altitude exceeded above 500 m (Fig. 7B). The coronarin D content was quite low (< 0.175) at lower altitude (< 50 m) and soil having low to moderate nitrogen content (< 220 mg/kg). The effect of manganese and altitude on content of coronarin D is shown in Fig. 7C. Coronarin D content was high at lower manganese content (< 12 mg/kg) in the soil and at higher altitudes (> 400 m). The effect of pH and altitude on coronarin D content was also observed in Fig. 7D. Acidic to neutral soil and elevation above 200 m favored coronarin D content. There was a slight decrease in content of coronarin D in alkaline rich soils. The influence of zinc and altitude on coronarin D content is shown in Fig. 8A. There was not much remarkable effect of zinc on coronarin D content, though higher elevation favored coronarin D content. The response surface plot of manganese and iron on content of coronarin D was shown in Fig. 8B. There was a decrease in content of coronarin D with increase in content of manganese and iron in the soil. High coronarin D content was observed in the range of 0 – 16 mg/kg of manganese and 0 – 20 mg/kg of iron. The response surface plot for manganese and zinc on coronarin D content is exhibited in Fig. 8C. Good content of coronarin D was observed in soil having low content of manganese and zinc. There was a gradual decrease in coronarin D content with increase in zinc content in the soil. The response of manganese and nitrogen on coronarin D is shown in Fig. 8D. At high nitrogen level (> 280 mg/kg) and with low to moderate amount of manganese (0 – 12 mg/kg), the content of coronarin D was high. Similarly, the effect of manganese and pH on coronarin D content was shown in Fig. 9A. There was not much variation in content of coronarin D with respect to pH, whereas there was a gradual decrease in content of coronarin D with increase in manganese levels in soil. The response surface plot of zinc and iron on coronarin D content is shown in Fig. 9B. There was a gradual decrease in the content of coronarin D with increase in iron and zinc content in the soil. Similar trend was observed

hotpaper.net

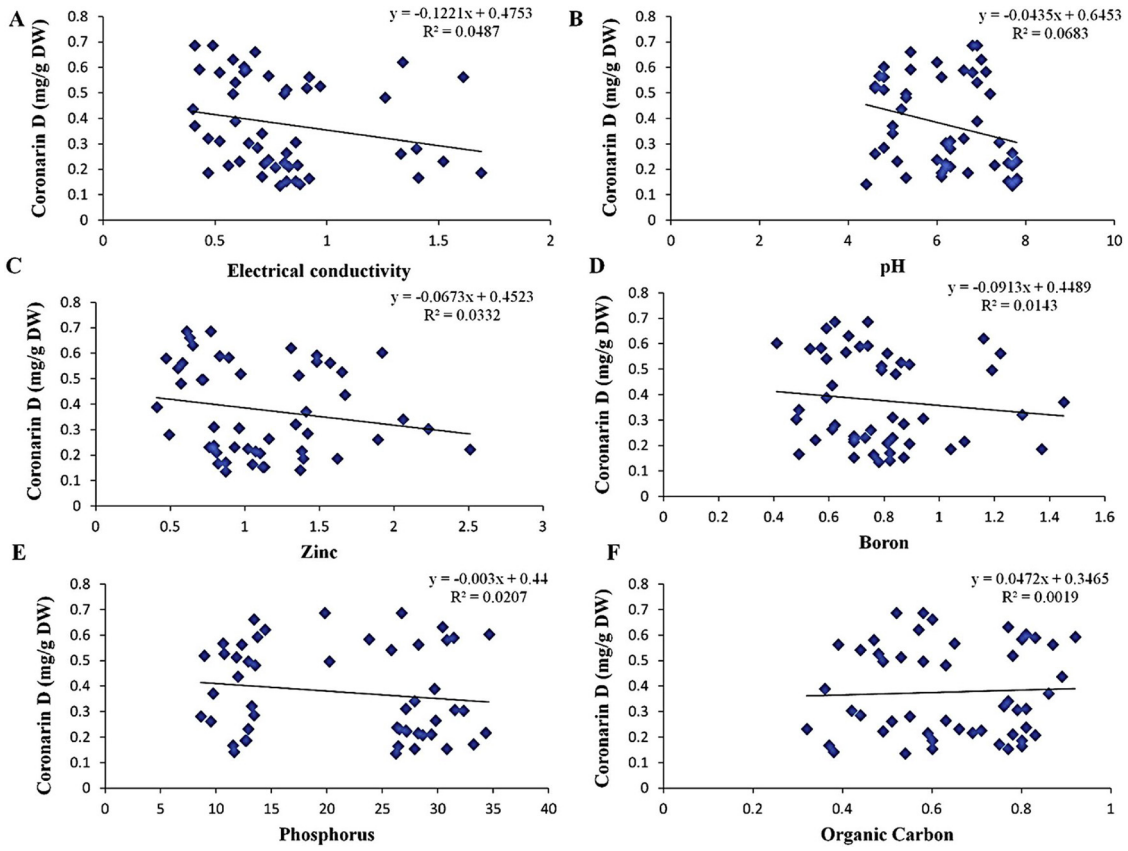

Fig. 6. Scatter plot matrix showing correlation of different soil parameters with coronarin D content. (A) Electrical conductivity; (B) pH; (C) Zinc; (D) Boron; (E) Phosphorus and (F) Organic carbon.

when nitrogen and zinc was considered together (Fig. 9C). The coronarin D content was high when the level of nitrogen is high (320–360 kg/ha) and zinc contents are low (< 0.6 mg/kg) in the soil. The influence of pH and zinc on coronarin D content was observed from Fig. 9D. The content of coronarin D was high in soils that are acidic in nature (pH < 6) and contains moderate to high amount of zinc (> 1 mg/kg). The effect of iron and nitrogen on coronarin D content is explained in Fig. 10A. High coronarin D content was observed in soils having nitrogen content in the range of 320 − 360 kg/ha. For the said nitrogen content, coronarin D content gradually declined from 0 to 1 5 mg/kg of iron, thereafter did not showed any change till 40 mg/kg and then start increasing. The response surface plot of coronarin D content against iron and pH is shown in Fig. 10B. The content of coronarin D decreased with increase in iron content, whereas pH had hardly any effect on coronarin D content. The influence of nitrogen and pH on coronarin D content was shown in Fig. 10C. The content of coronarin D was high in acidic soils (pH < 5) having low nitrogen levels (< 160 kg/ha) and at slightly acidic to alkaline soils (pH 6–8) rich in nitrogen (> 320 kg/ha).

3.4. Sensitivity analysis

The detailed description of sensitivity analysis is illustrated in Table 10. Sensitivity analysis is carried out to analyze the variables that are affecting the neural network model output by varying the value of model parameters and changing it structure. The eff ;ects of the input variables to predict coronarin D content in ANN model was ranked from the highest to lowest in Table 10. From the Table 10, it can be observed that altitude had the highest influence on coronarinD content with an error ratio of 3.648. The next sensitive parameters were manganese, zinc, iron, nitrogen and pH with an error ratio of 3.284, 2.541, 2.166, 2.140 and 2.135, respectively. Maximum average temperature, potassium, sulphur and copper had reasonable influence on coronarinD content having error ratio of 2.076, 1.911, 1.616 and 1.549. Increased error ratios indicate more influential parameters. The least influential factors were organic carbon, phosphorus, electrical conductivity, minimum average temperature, average relative humidity, boron, precipitation and average temperature.

3.5. Optimization of coronarin D content

As per the finding of the current study, content of coronarin D in *Hedychium coronarium* can be increased by managing soil nutrients at a specific site. An example of optimization of coronarin D content has been illustrated in Fig. 11, where parameters like altitude, zinc and manganese were changed to study the effect on coronarin D content. Altitude was changed from 0.211 to 0.222, zinc was changed from 0.922 to 0.961, and manganese was changed from 0.255 to 0.283. By modifying these three parameters, the coronarin D content increased to 0.732 from 0.667 mg/100 mg dry wt developed by neural network model.

3.6. Application of ANN model for prediction of coronarin D content at a new location

ANN model can be applied for predicting the coronarin D content at an unknown/new site. The developed model could exhibit accuracy near to 90 % to the experimental value when applied at a new site. The developed model without training was tested at Rajini (Khurdha) and it predicted the coronarin D value to be 0.667 mg/100 mg dry wt. which is close to the experimental value of 0.602 mg/100 mg dry wt. Thus the study demonstrated that ANN model can give satisfactory prediction performance of coronarin D content using climatic and edaphic data.

hotpaper.net

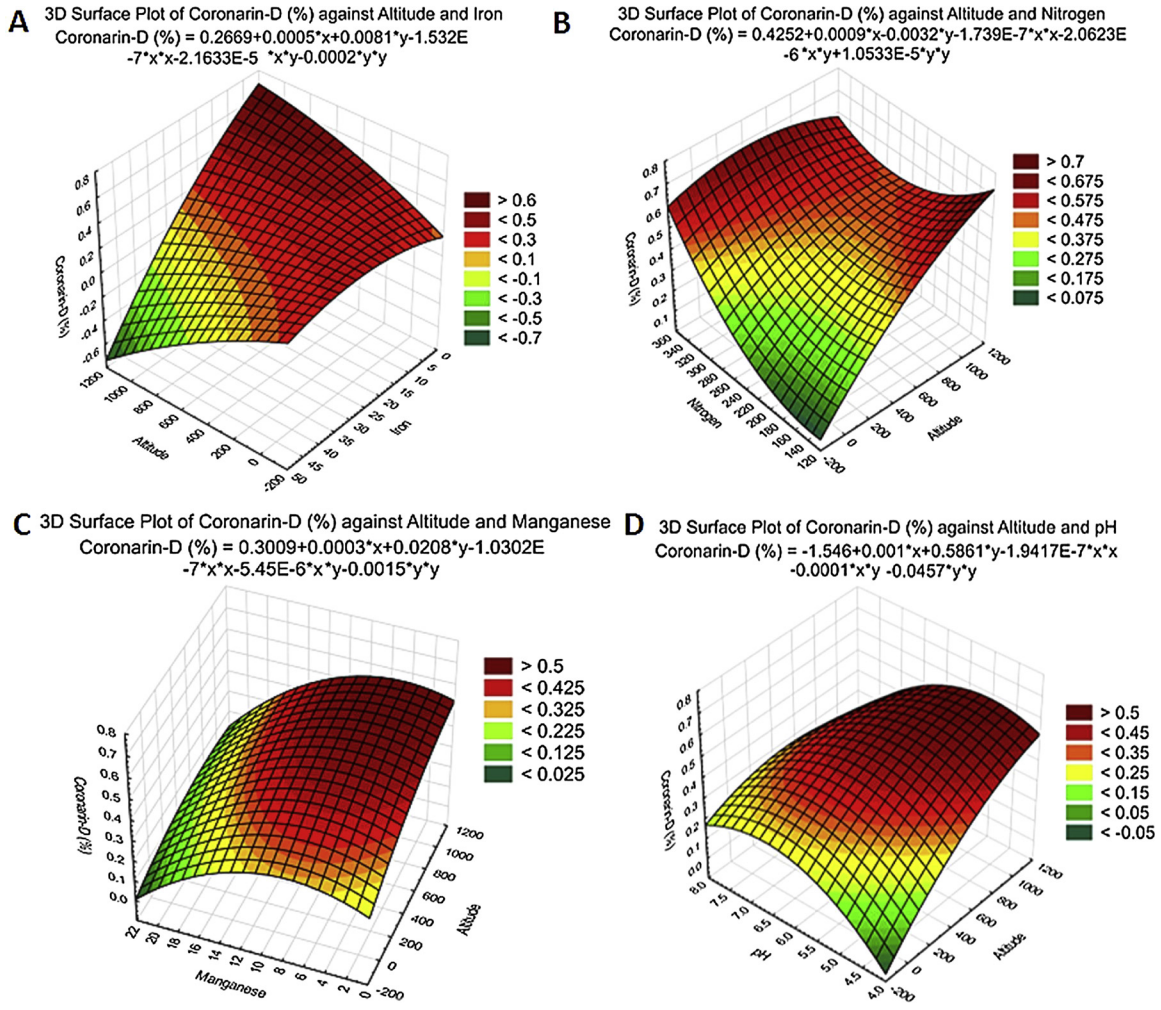

Fig. 7. Response surface plots for coronarin D content as a function of (A) Altitude v/s Iron; (B) Altitude v/s Nitrogen; (C) Altitude v/s Manganese and (D) Altitude v/s pH.

4. Discussion

Nowadays researchers are using artificial neural network (ANN) as predictive tools in an extensive range of disciplines, including agriculture and soil science (Park and Vlek, 2002; Somaratne et al., 2005). The superiority of ANN over other statistical modeling technique is that it does not infer a prior data structure, and can discern nonlinear relationships and complex interactions, thereby revealing an unknown relationship between input parameters (Alvarez, 2009). The flow of information occurs from the output layer to the input layer through the hidden layer by iterative tuning of weights. The learning process that is being carried out in multilayer perceptron (MLP) network is usually by back propagation algorithm method. The complexity of ANN model is determined by the number of hidden nodes. Presence of too many neurons will lead to data overfitting (Kumar and Porkodi, 2009). MLP model with sigmoid axon transfer function has been used by many researchers to predict the performance of diff ;erent crops (Abdipour et al., 2018; Emamgholizadeh et al., 2015). Four statistical quality parameters, including root mean square error (RMSE), coefficient of determination (R^2), mean absolute error (MAE) and mean absolute percentage error (MAPE) were used to evaluate the ANN model performance. To find the appropriate number of hidden layers and neurons (best topology), the diff ;erent number of hidden layers (1–4) and neurons in each hidden layer (2–17) were tested through trial and error. The MLP model with sigmoid transfer function and five neurons in the hidden layer had the best performance due to the least MAE and RMSE and the highest R^2 values in both training and testing stages. A low MAPE value was obtained for the ANN model based on the MLP network of the 18:5:1 structure, which was 4.87 % for training dataset. Sigmoid transfer function has been used by many researchers to predict the performance of diff ;erent crops (Abdipour et al., 2018; Emamgholizadeh et al., 2015). Rahman and Bala (2010) showed the ANN model consists of four layer network with two hidden layers as the best model for jute prediction. Sinha et al. (2012) designed an ANN model with three hidden layers for optimum dye extraction from pomegranate rind. Similarly, Abdipour et al. (2019) selected ANN topology with 5-5-4-1 architecture as the best model to predict seed yield of safflower.

In the present research, the ANN model developed showed good predictive capability for coronarin D as evaluated by its statistical parameters such as correlation coefficient (R^2) and root mean square error (RMSE) values. The developed model gave a higher R^2 value of 0.891 and a lower RMSE value of 0.06 for training data set which imply that there is less deviation between the experimental and predicted values. The closer the R^2 value to 1 and lesser the RMSE value, the stronger the ANN model. As a result, it may be concluded that the model predicted for coronarin D content in *H. coronarium* is quite accurate. A similar study showing high predictive analysis of ANN model has been earlier reported wherein the error values of ANN model was less as compared to response surface methodology (RSM) model (Sodeifian et al., 2016).

A response surface plot is a graph that helps us to understand the

hotpaper.net

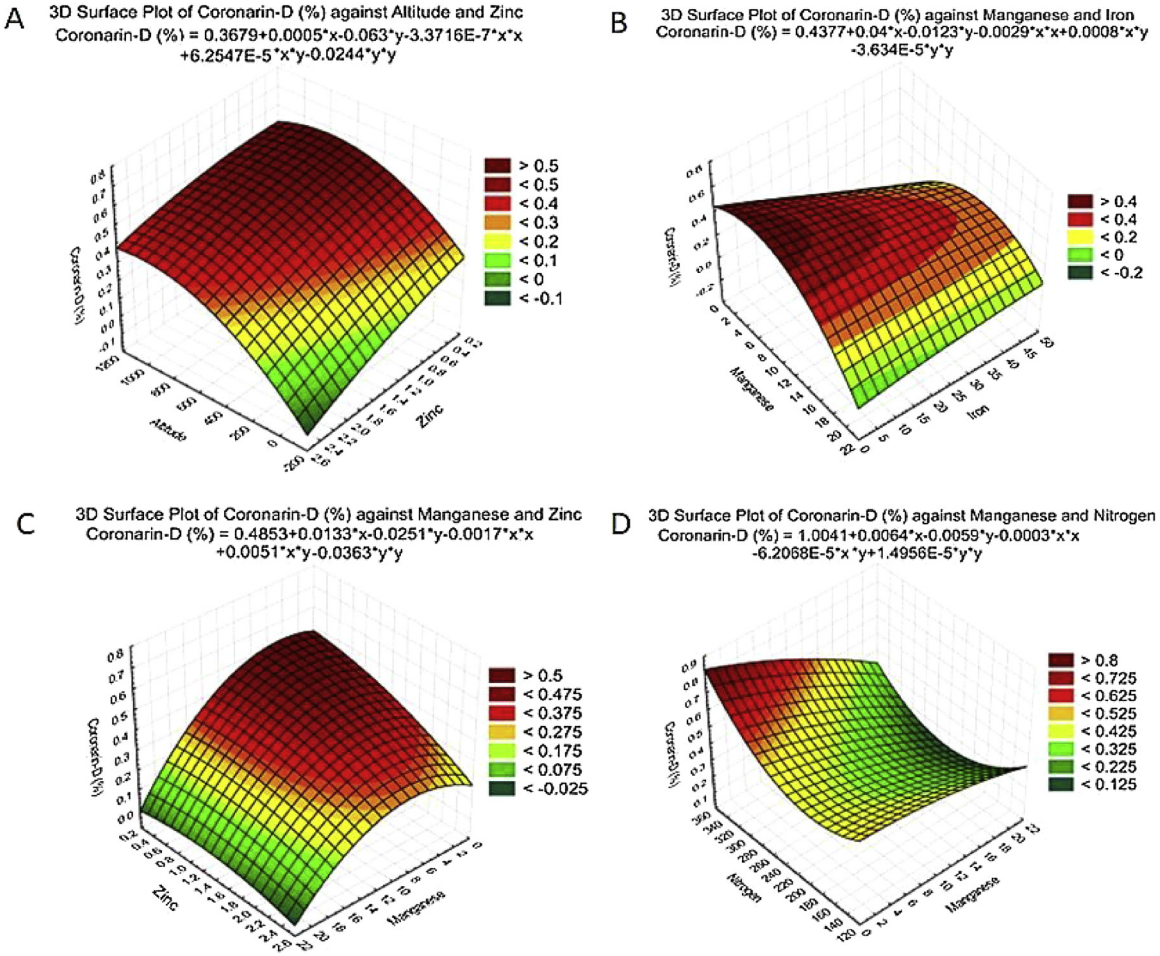

Fig. 8. Response surface plots for coronarin D content as a function of (A) Altitude v/s Zinc; (B) Manganese v/s Iron; (C) Manganese v/s Zinc and (D) Manganese v/s Nitrogen.

relationship between two dependent variables on the response of the independent variable. It creates a mathematical model that represents the biochemical activity (Baş and Boyacı, 2007). Several reports have applied response surface methodology (RSM) to predict optimum extraction conditions for maximum recovery of various phytoconstituents such as saponin from ginseng roots (Kwon et al., 2003), sugar from spent coffee (Mussatto et al., 2011), polyphenols from fruit of *Feronia limonia* (Ilaiyaraja et al., 2015).

Sensitivity analysis approach is used in the ANN model to identify the effect of input parameters on the output of the model. It will help us to find out the input parameters that causes the most disturbances in the performance of the ANN model. This type of analysis will help us to investigate the highly sensitive input environmental and soil factors on predicting the content of coronarin D. The most influential parameter was altitude with an error ratio of 3.648. Higher error ratios correspond to increased predictive error for all compounds upon removal of this parameter from the dataset. Error ratios greater than 1 indicate more important parameter. Previous study have also showed that descriptor like altitude is influential for modelling secondary metabolite content (Akbar et al., 2016). ANN model was used to determine the effect of soil moisture and salinity on sunflower growth, seed and oil yield (Dai et al., 2011). The sensitivity analysis showed that for low to medium salinity soils, sensitivity of sunflower yield was highest at crop squaring stage, whereas for higher salinity soils sensitivity was highest at seedling stage. Similarly in another study sensitivity analysis have shown number of capsules per plant to be the most influential factor determining safflower yield (Abdipour et al., 2019). Desai et al. (2008) studied the effect of fermentation media concentrations on the yield of biopolymer scleroglucan using ANN model. Sensitivity analysis revealed that glucose has the highest influence on yield of scleroglucan, whereas other media components such as yeast extract, magnesium sulphate and dipotassium hydrogen phosphate had the least influence.

This is the first study representing the effect of environmental and soil nutrient factors on content of coronarin D in *H. coronarium* sampled from five provinces of India. The study revealed that a combination of two or more factor has more influence on coronarin D content than a single factor. The present study showed that variation in coronarin D content can be attributed to environmental variables, soil macronutrients and micronutrients. Difference in secondary metabolite content in plants are related to edaphic factors, geographic and physiological variations, genetic variability, seasonal variation, plant age and other biological factors (Figueiredo et al., 2008). Our result is in close agreement with Liu et al. (2016), who have studied the role of environmental parameters on the active content of *Potentilla fruticosa* L. from different parts of China and found that contents of certain substances were significantly higher under specific environments. Alam and Naik (2009) have shown that podophyllotoxin content in the root of *P. hexandrum* increases above 6.62 % when pH, organic carbon and nitrogen content in soil were higher than 4.82, 3.23 and 2.7 % respectively. Similarly, Akbar et al. (2016) have also demonstrated that curcumin content in the rhizome of *C. longa* is high when nitrogen content and pH in the soil are high. Out of 50 *H. coronarium* accessions screened in the present research, six genotypes (HC23, HC30, HC32, HC34, HC39, HC48) exhibited coronarin D content greater than 0.5 mg/100 mg dry wt. These high yielding coronarin D accessions of *H. coronarium* can be bring under cultivations for commercial production

hotpaper.net

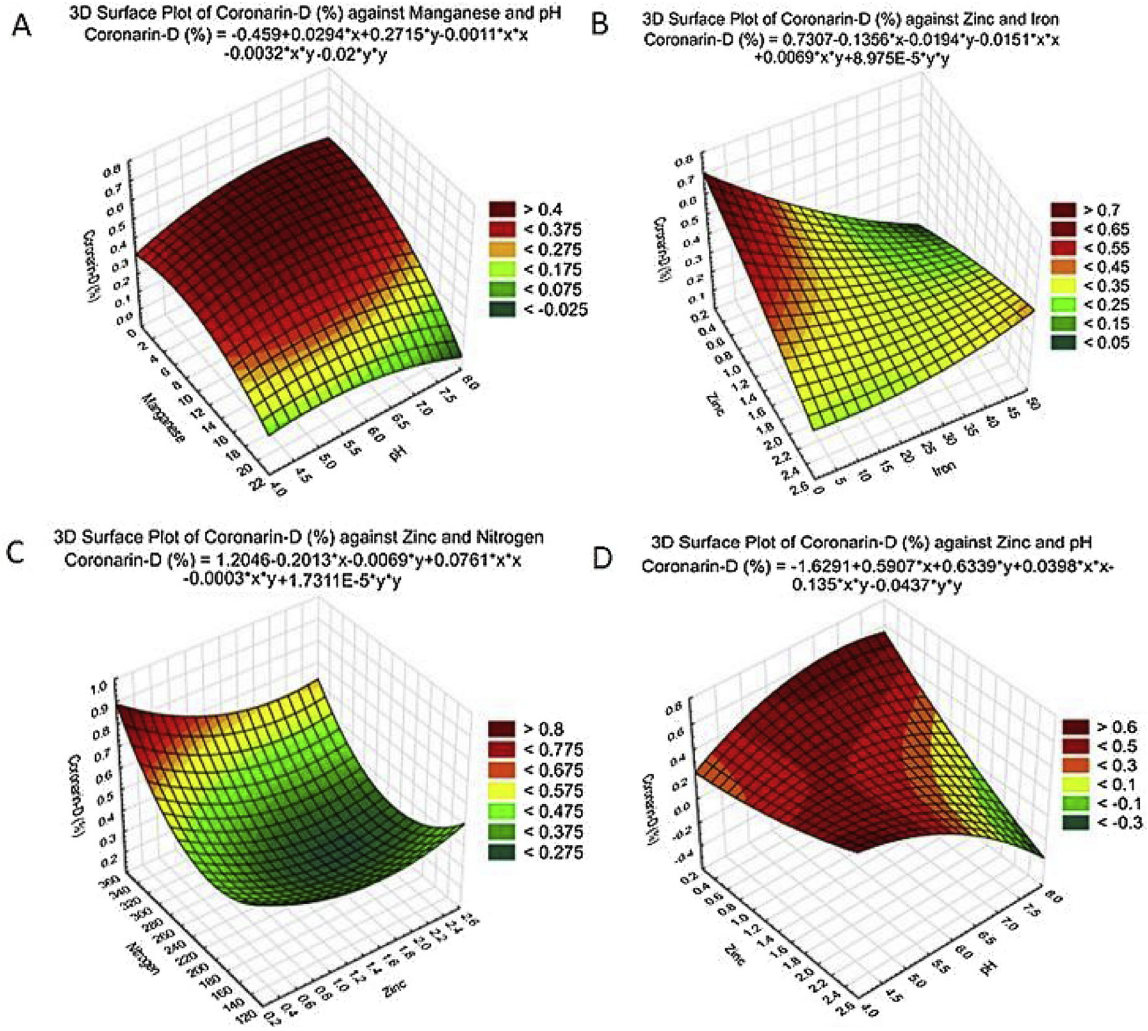

Fig. 9. Response surface plots for coronarin D content as a function of (A) Manganese v/s pH; (B) Zinc v/s Iron; (C) Zinc v/s Nitrogen and (D) Zinc v/s pH.

and further multilocational trials can be conducted in order to validate their high yield.

Micronutrients play a central role in plant metabolism and are essential for their growth. Micronutrients are a group of elements that usually occur in minute quantities in the soil. Compositional changes in micronutrient in soil may also bring about qualitative changes in the plant. Micronutrients interact with organic compounds forming metal-ligand complexes. Application of micronutrients enhances photosynthetic and other metabolic activity, thereby leading to an increase in various plant metabolites. The present study showed that increase content of potassium also favored the coronarin D content. Potassium is a crucial micronutrient that activates certain enzymes that are crucial in maintaining water balance in plants (Wang et al., 2013). Potassium performs various plant enzyme functions and is needed for metabolite pattern of higher plants (Marschner, 2011). Generally, crop yields are greatly reduced in potassium deficient soils. Study has shown that increased application of potassium showed an increase in free amino acids content in tea leaves (Ruan et al., 1998). Another soil factor significantly affecting the coronarin D content is iron. Iron act as a key enzymes of electron transport chain and is needed to maintain chloroplast structure (Rout and Sahoo, 2015).

Medicinal plants have greater medicinal efficacy in their natural habitat. Change in the natural habitat adversely affects the production of bioactive compounds. Soil properties and environmental factors must be quite similar to natural habitat. Selection of cultivated land chosen for the growth of *H. coronarium* should have similar soil properties and environment as natural habitat in order to mimic the natural condition that is ideal for *H. coronarium* to produce high coronarin D content. This can be achieved by soil management programme and by adding nutrient factors to the soil.

The current study revealed that coronarin D content can be optimized in the ANN model by changing altitude, manganese, zinc and iron content in the soil. Additionally, production of secondary metabolites in plants is an intricate physiological process. Several factors like plant age, seasons, genetic and environmental factors affect its metabolite content. Nonetheless, it is understood that the differences in coronarin D content in *H. coronarium* are affected by above said factors, which needs to be explored further. The ANN model was used for predicting coronarin D content in *H. coronarium* at a new location. The coronarin D content predicted value was found to be 0.667 mg/100 mg dry wt. at a location Rajini, Odisha which is close to the experimental value (0.602 mg/100 mg dry wt.).

5. Conclusions

In the current study, optimal ANN model determined for prediction and optimization of coronarin D content showed multilayer perceptron (MLP) neural network with five neurons in hidden layer to have superior performance with regression value of 0.891. ANN model revealed that the coronarin D content of *H. coronarium* could be enhanced from 0.667 % to 0.732 % by varying sensitive parameters (Altitude, zinc and manganese content) of the model. The results showed the

hotpaper.net

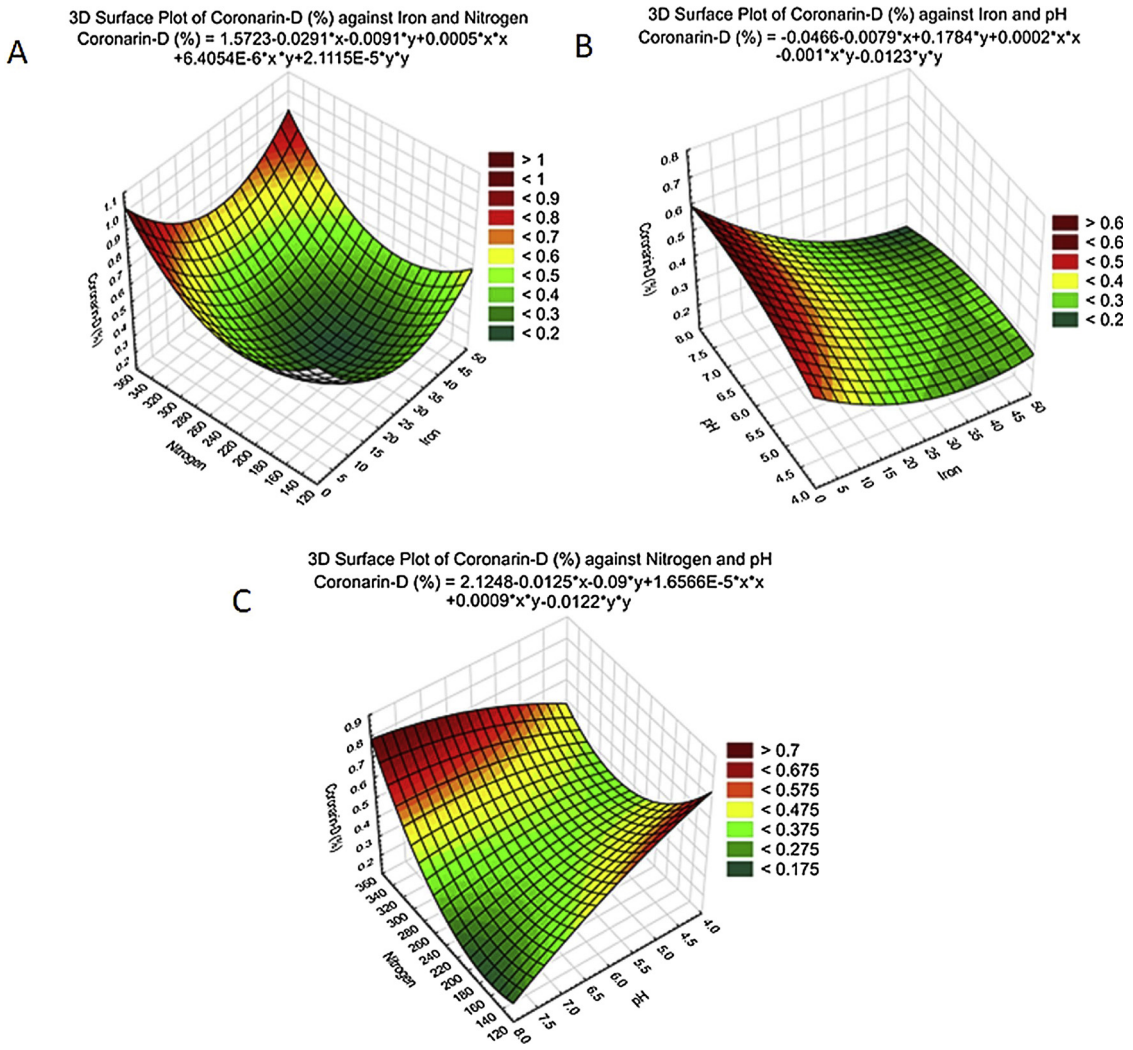

Fig. 10. Response surface plots for coronarin D content as a function of (A) Iron v/s Nitrogen; (B) pH v/s Iron and (C) Nitrogen v/s pH.

Table 10
Sensitivity analysis of neural network.

Parameters	Error quotient	Rank
Altitude	3.648	1
Manganese	3.284	2
Zinc	2.541	3
Iron	2.166	4
Nitrogen	2.140	5
pH	2.135	6
Maximum average temperature	2.076	7
Potassium	1.911	8
Sulphur	1.616	9
Copper	1.549	10
Precipitation	1.440	11
Electrical conductivity	1.386	12
Average annual temperature	1.369	13
Phosphorus	1.313	14
Minimum average temperature	1.180	15
Organic carbon	1.175	16
Boron	1.107	17
Average relative humidity	1.034	18

possibility to predict coronarin D content using a combination of topographic, soil and environmental data which was unstudied so far. However it is assumed that variation in coronarin D content is dependent on altitude, manganese, zinc, iron and nitrogen, which needs further research. The developed model could provide suitable information regarding the site selection and optimization of soil and environmental factors to increase the content of coronarin D that can be used for planning any conservation aspects.

Credit authorship contribution statement

AR performed the experiments, collected the data, analyzed the data and wrote the manuscript. TH and SJ participated in the HPTLC analysis of the extracts. AS performed the statistical analysis. SM and NM supervised the work and participated in the drafting of the manuscript. SN and BG conceived the idea of this work and obtained funding for the research. All authors read and approved the final manuscript.

Declaration of Competing Interest

The authors declare that they have no known competing financial interests or personal relationships that could have appeared to influence the work reported in this paper.

Acknowledgements

The authors would like to thank Department of Biotechnology (No: BT/PR7953/PBD/17/855/2013), Ministry of Science and Technology, Government of India for their financial support.

hotpaper.net

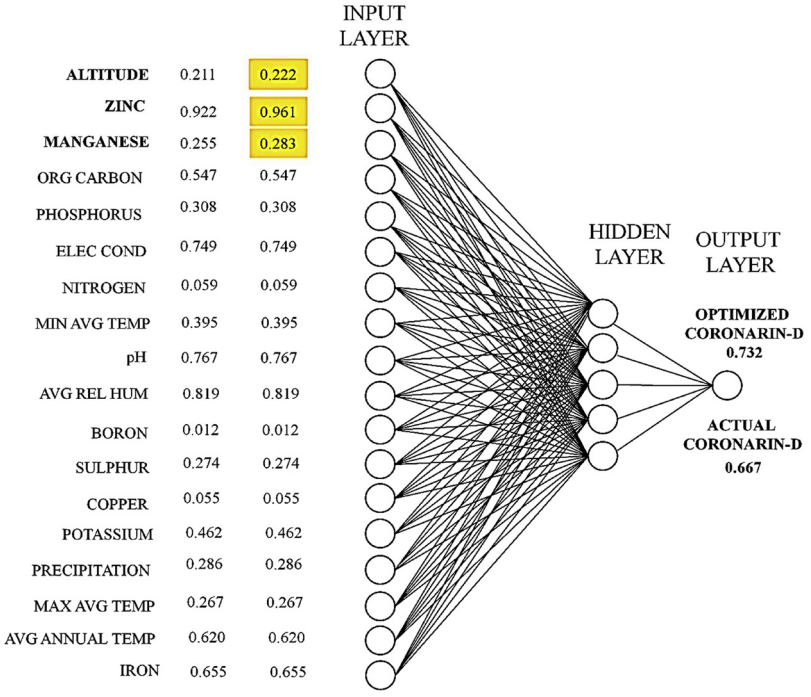

Fig. 11. Optimization of coronarin D content by changing input parameters of ANN model.

Appendix A. Supplementary data

Supplementary material related to this article can be found, in the online version, at doi:https://doi.org/10.1016/j.indcrop.2020.112186.

References

Abdipour, M., Ramazani, S.H.R., Younessi-Hmazekhanlu, M., Niazian, M., 2018. Modeling oil content of sesame (*Sesamum indicum* L.) using artificial neural network and multiple linear regression approaches. J. Am. Oil Chem. Soc. 95, 283–297.

Abdipour, M., Younessi-Hmazekhanlu, M., Ramazani, S.H., 2019. Artificial neural networks and multiple linear regression as potential methods for modeling seed yield of safflower (*Carthamus tinctorius* L.). Ind. Crops Prod. 127, 185–194.

Ahmadi, S.H., Sepaskhah, A.R., Andersen, M.N., Plauborg, F., Jensen, C.R., Hansen, S., 2014. Modeling root length density of field grown potatoes under diff ;erent irrigation strategies and soil textures using artificial neural networks. Field Crops Res. 162, 99–107.

Akbar, A., Kuanar, A., Joshi, R.K., Sandeep, I.S., Mohanty, S., Naik, P.K., Mishra, A., Nayak, S., 2016. Development of prediction model and experimental validation in predicting the curcumin content of turmeric (*Curcuma longa* L.). Front. Plant Sci. 7, 1507.

Akbar, A., Kuanar, A., Patnaik, J., Mishra, A., Nayak, S., 2018. Application of Artificial Neural Network modeling for optimization and prediction of essential oil yield in turmeric (*Curcuma longa* L.). Comput. Electron. Agr. 148, 160–178.

Alam, M.A., Naik, P.K., 2009. Impact of soil nutrients and environmental factors on podophyllotoxin content among 28 *Podophyllum hexandrum* populations of northwestern Himalayan region using linear and nonlinear approaches. Comm. Soil. Sci. Plant. Ana. 40, 2485–2504.

Alvarez, R., 2009. Predicting average regional yield and production of wheat in the Argentine Pampas by an artificial neural network approach. Eur. J.Agron. 30, 70–77.

Baş, D., Boyacı, İ., 2007. Modeling and optimization II: comparison of estimation capabilities of response surface methodology with artificial neural networks in a biochemical reaction. J. Food Eng. 78, 846–854.

Bray, R.H., Kurtz, L.T., 1945. Determination of total, organic, and available forms of phosphorus in soils. Soil Sci. 59, 39–46.

Bremner, J.M., Mulvaney, C.S., 1982. Nitrogen - total. In: Page, A.L., Miller, R.H., Keeney, D.K. (Eds.), Methods Of Soil Analysis. Part 2 - Chemical and Microbiological Properties. Soil Science of America, Inc., Wisconsin, pp. 595–616.

Céline, V., Adriana, P., Eric, D., Joaquina, A.C., Yannick, E., Augusto, L.F., Rosario, R., Dionicia, G., Michel, S., Denis, C., Geneviève, B., 2009. Medicinal plants from the Yanesha (Peru): evaluation of the leishmanicidal and antimalarial activity of selected extracts. J. Ethnopharmacol. 123, 413–422.

Chan, E.W., Wong, S.K., 2015. Phytochemistry and pharmacology of ornamental gingers, *Hedychium coronarium* and *Alpinia purpurata*: a review. J. Integr. Med. 13, 368–379.

Chen, J.J., Ting, C.W., Wu, Y.C., Hwang, T.L., Cheng, M.J., Sung, P.J., Wang, T.C., Chen, J.F., 2013. New labdane-type diterpenoids and anti-inflammatory constituents from *Hedychium coronarium*. Int. J. Mol. Sci. 14, 13063–13077.

Chen, J.C., Hsieh, M.C., Lin, S.H., Lin, C.C., His, Y.T., Lo, Y.S., Chuang, Y.C., Hsieh, M.J., Chen, M.K., 2017. Coronarin D induces reactive oxygen species-mediated cell death in human nasopharyngeal cancer cells through inhibition of p38 MAPK and activation of JNK. Oncotarget. 8, 108006–108019.

Chimnoi, N., Sarasuk, C., Khunnawutmanotham, N., Intachote, P., Seangsai, S., Saimanee, B., Pisutjaroenpong, S., Mahidol, C., Techasakul, S., 2009. Phytochemical re-investigation of labdane-type diterpenes and their cytotoxicity from the rhizomes of *Hedychium coronarium*. Phytochem. Lett. 2, 184–187.

Dai, X., Huo, Z., Wang, H., 2011. Simulation for response of crop yield to soil moisture and salinity with artificial neural network. Field. Crop. Res. 121, 441–449.

Desai, K.M., Survase, S.A., Saudagar, P.S., Lele, S.S., Singhal, R.S., 2008. Comparison of artificial neural network (ANN) and response surface methodology (RSM) in fermentation media optimization: case study of fermentative production of scleroglucan. Biochem. Eng. J. 41, 266–273.

Donipati, P., Sreeramulu, D.S., 2015. *In vitro* anticancer activity of *Hedychium coronarium* against human breast cancer cell line MCF-7. Int. J. Adv. Res. 3, 1497–1501.

Emamgholizadeh, S., Parsaeian, M., Baradaran, M., 2015. Seed yield prediction of sesame using artificial neural network. Eur. J. Agron. 68, 89–96.

Fieuzal, R., Sicre, C.M., Baup, F., 2017. Estimation of corn yield using multi-temporal optical and radar satellite data and artificial neural networks. Int. J. Appl. Earth Obs. Geoinf. 57, 14–23.

Figueiredo, A.C., Barroso, J.G., Pedro, L.G., Scheffer, J.J., 2008. Factors affecting secondary metabolite production in plants: volatile components and essential oils. Flavour Fragr. J. 23, 213–226.

Gairola, S., Shariff, N.M., Bhatt, A., 2010. Influence of climate change on production of secondary chemicals in high altitude medicinal plants: issues needs immediate attention. J. Med. Plant Res. 4, 1825–1829.

Ilaiyaraja, N., Likhith, K.R., Babu, G.S., Khanum, F., 2015. Optimisation of extraction of bioactive compounds from *Feronia limonia* (wood apple) fruit using response surface methodology (RSM). Food Chem. 173, 348–354.

Kaomongkolgit, R., Jamdee, K., Wongnoi, S., Chimnoi, N., Techasakul, S., 2012. Antifungal activity of coronarin D against *Candida albicans*. Oral Surg. Oral Med. Oral Pathol. Oral Radiol. 114, 61–66.

Kazem, H.A., Yousif, J.H., 2017. Comparison of prediction methods of photovoltaic power system production using a measured dataset. Energy Convers. Manage. 148, 1070–1081.

Kumar, K.V., Porkodi, K., 2009. Modelling the solid–liquid adsorption processes using artificial neural networks trained by pseudo second order kinetics. Chem. Eng. J. 148, 20–25.

Kunnumakkara, A.B., Ichikawa, H., Anand, P., Mohankumar, C.J., Hema, P.S., Nair, M.S., Aggarwal, B.B., 2008. Coronarin D, a labdane diterpene, inhibits both constitutive and inducible nuclear factor-κB pathway activation, leading to potentiation of apoptosis, inhibition of invasion, and suppression of osteoclastogenesis. Mol. Cancer Ther. 7, 3306–3317.

Kwon, J.H., Bélanger, J.M., Paré, J.J., 2003. Optimization of microwave-assisted extraction (MAP) for ginseng components by response surface methodology. J. Agric. Food Chem. 51, 1807–1810.

Lin, H.W., Hsieh, M.J., Yeh, C.B., Hsueh, K.C., Hsieh, Y.H., Yang, S.F., 2018. Coronarin D induces apoptotic cell death through the JNK pathway in human hepatocellular carcinoma. Environ. Toxicol. 33, 946–954.

Lindsay, W.L., Norvell, W.A., 1978. Development of a DTPA soil test for zinc, iron,

hotpaper.net

manganese, and copper 1. Soil Sci. Soc. Am. J. 42, 421–428.
Liu, W., Yin, D., Li, N., Hou, X., Wang, D., Li, D., Liu, J., 2016. Influence of environmental factors on the active substance production and antioxidant activity in *Potentilla fruticosa* L. and its quality assessment. Sci. Rep. 6, 28591.
Marschner, H., 2011. Marschner's Mineral Nutrition of Higher Plants. Academic press.
Matsuda, H., Morikawa, T., Sakamoto, Y., Toguchida, I., Yoshikawa, M., 2002. Labdane-type diterpenes with inhibitory effects on increase in vascular permeability and nitric oxide production from *Hedychium coronarium*. Bioorg. Med. Chem. 10, 2527–2534.
Matsumura, K., Gaitan, C.F., Sugimoto, K., Cannon, A.J., Hsieh, W.W., 2015. Maize yield forecasting by linear regression and artificial neural networks in Jilin, China. J. Agric. Sci. 153, 399–410.
Michelon, G.K., de Menezes, P.L., Bazzi, C.L., Jasse, E.P., Magalhães, P.S., Borges, L.F., 2018. Artificial neural networks to estimate the productivity of soybeans and corn by chlorophyll readings. J. Plant Nutr. 41, 1285–1292.
Miller, T.H., Gallidabino, M.D., MacRae, J.I., Owen, S.F., Bury, N.R., Barron, L.P., 2019. Prediction of bioconcentration factors in fish and invertebrates using machine learning. Sci. Total Environ. 648, 80–89.
Mohammadi, S., Siosemarde, M., 2016. Application of artificial neural networks in order to predict Mahabad River discharge. Open J. Ecol. 6, 427.
Moradi, G., Dehghani, S., Khosravian, F., Arjmandzadeh, A., 2013. The optimized operational conditions for biodiesel production from soybean oil and application of artificial neural networks for estimation of the biodiesel yield. Renew. Energy 50, 915–920.
Morikawa, T., Matsuda, H., Sakamoto, Y., Ueda, K., Yoshikawa, M., 2002. New farnesane-type sesquiterpenes, hedychiols A and B 8, 9-diacetate, and inhibitors of degranulation in RBL-2H3 cells from the rhizome of *Hedychium coronarium*. Chem. Pharm. Bull. 50, 1045–1049.
Mussatto, S.I., Carneiro, L.M., Silva, J.P., Roberto, I.C., Teixeira, J.A., 2011. A study on chemical constituents and sugars extraction from spent coffee grounds. Carbohydr. Polym. 83, 368–374.
Nelson, D.W., Sommers, L., 1982. Total carbon, organic carbon, and organic matter 1. In: Page, A.L., Miller, R., Keeney, D.K. (Eds.), Methods of Soil Analysis. Part 2. Chemical and Microbiological Properties. Soil Science of America, Inc., Winconsin, pp. 539–579.
Oh, S., Jeong, I.H., Shin, W.S., Wang, Q., Lee, S., 2006. Synthesis and biological activity of (+)-hedychilactone A and its analogs from (+)-sclareolide. Bioorg. Med. Chem. Lett. 16, 1656–1659.
Pachurekar, P., Dixit, A.K., 2017. A review on pharmacognostical phytochemical and ethnomedicinal properties of *Hedychium coronarium* J. Koenig an endangered medicine. Int. J. Chin. Med. 1, 49–61.
Page, A.L., Miller, R.H., Keeney, D.R., 1982. Methods of Soil Analysis, Part 2: Chemical and Microbiological Properties, 2nd ed. ASA and SSSA, Madison, Wisconsin.
Parida, R., Mohanty, S., Nayak, S., 2015. Chemical composition of essential oil from leaf and rhizome of micropropagated and conventionally grown *Hedychium coronarium* Koen. from Eastern India. J. Essent. Oil. Bear. Pl. 18, 161–167.
Park, S.J., Vlek, P.L., 2002. Environmental correlation of three-dimensional soil spatial variability: a comparison of three adaptive techniques. Geoderma 109, 117–140.
Rahman, M.M., Bala, B.K., 2010. Modelling of jute production using artificial neural networks. Biosyst. Eng. 105, 350–356.
Ray, A., Dash, B., Sahoo, A., Nasim, N., Panda, P.C., Patnaik, J., Ghosh, B., Nayak, S., Kar, B., 2017. Assessment of the terpenic composition of *Hedychium coronarium* oil from Eastern India. Ind. Crop. Prod. 97, 49–55.
Ray, A., Jena, S., Dash, B., Kar, B., Halder, T., Chatterjee, T., Ghosh, B., Panda, P.C., Nayak, S., Mahapatra, N., 2018. Chemical diversity, antioxidant and antimicrobial activities of the essential oils from Indian populations of *Hedychium coronarium* Koen. Ind. Crop. Prod. 112, 353–362.
Reuk-ngam, N., Chimnoi, N., Khunnawutmanotham, N., Techasakul, S., 2014. Antimicrobial activity of coronarin D and its synergistic potential with antibiotics. Biomed Res. Int. 2014.
Rout, G.R., Sahoo, S., 2015. Role of iron in plant growth and metabolism. Rev. Agric. Sci. 3, 1–24.
Ruan, J., Wu, X., Ye, Y., Härdter, R., 1998. Effect of potassium, magnesium and sulphur applied in different forms of fertilisers on free amino acid content in leaves of tea (*Camellia sinensis* L). J. Sci. Food Agric. 76, 389–396.
Singh, A., Imtiyaz, M., Isaac, R.K., Denis, D.M., 2012. Comparison of soil and water assessment tool (SWAT) and multilayer perceptron (MLP) artificial neural network for predicting sediment yield in the Nagwa agricultural watershed in Jharkhand, India. Agric. Water Manag. 104, 113–120.
Sinha, K., Saha, P.D., Datta, S., 2012. Response surface optimization and artificial neural network modeling of microwave assisted natural dye extraction from pomegranate rind. Ind. Crop. Prod. 37, 408–414.
Sodeifian, G., Sajadian, S.A., Ardestani, N.S., 2016. Optimization of essential oil extraction from *Launaea acanthodes* Boiss: Utilization of supercritical carbon dioxide and cosolvent. J. Supercrit. Fluid. 116, 46–56.
Somaratne, S., Seneviratne, G., Coomaraswamy, U., 2005. Prediction of soil organic carbon across different land-use patterns. Soil Sci. Soc. Am. J. 69, 1580–1589.
Van Kiem, P., Thuy, N.T., Anh, H.L., Nhiem, N.X., Van Minh, C., Yen, P.H., Ban, N.K., Hang, D.T., Tai, B.H., Van Tuyen, N., Mathema, V.B., 2011. Chemical constituents of the rhizomes of *Hedychium coronarium* and their inhibitory effect on the pro-inflammatory cytokines production LPS-stimulated in bone marrow-derived dendritic cells. Bioorg. Med. Chem. Lett. 21, 7460–7465.
Wang, A., 2018. Establishment of wheat yield prediction model in dry farming area based on neural network. NeuroQuantology 16, 768–775.
Wang, M., Zheng, Q., Shen, Q., Guo, S., 2013. The critical role of potassium in plant stress response. Int. J. Mol. Sci. 14, 7370–7390.